

Relativistic Mirrors in Laser Plasmas (Analytical Methods)

S. V. Bulanov^{1,2}, T. Zh. Esirkepov¹, M. Kando¹, J. Koga¹

¹ Kansai Photon Science Institute, JAEA, 8-1-7 Umemidai, Kizugawa, Kyoto, 619-0215 Japan

²A. M. Prokhorov Institute of General Physics, Russian Academy of Sciences,

Vavilov street, 38, Moscow, 119991 Russia

(Dated: March 25, 2016)

Relativistic flying mirrors in plasmas are realized as thin dense electron (or electron-ion) layers accelerated by high-intensity electromagnetic waves to velocities close to the speed of light in vacuum. The reflection of an electromagnetic wave from the relativistic mirror results in its energy and frequency changing. In a counter-propagation configuration, the frequency of the reflected wave is multiplied by the factor proportional to the Lorentz factor squared. This scientific area promises the development of sources of ultrashort X-ray pulses in the attosecond range. The expected intensity will reach the level at which the effects predicted by nonlinear quantum electrodynamics start to play a key role.

PACS numbers: 52.27.Ny, 52.72.+v

Contents

I. Introduction	2
II. Relativistic Flying Mirror Concept for Electromagnetic Field Intensification and Frequency Upshifting	3
A. Reflection of Electromagnetic Wave from Relativistic Mirror Moving with the Constant Velocity	3
B. Light Reflection at the Receding Mirror and Ion acceleration by the Radiation Pressure	5
C. Light Reflection at the Accelerated Mirror	5
III. Thin Electron Layer as a Relativistic Mirror	7
A. Light Reflection at the Oscillating Mirror	8
B. Reflection Coefficient of Electromagnetic Radiation from a Thin Electron Layer	9
C. Relativistic Transparency of a Thin Plasma Layer	11
IV. Nonlinear plasma waves as relativistic mirrors	13
A. Plasma Oscillations Excited in Near-Critical Inhomogeneous Plasma	13
B. Nonlinear Wake Wave Excited by a Short Laser Pulse in Underdense Plasmas	14
C. Above-Barrier Reflection from Caustics Formed by Breaking Plasma Waves	16
V. Compact Source of High-Brightness X-Rays Based on the Mechanism of a Relativistic Flying Mirror	17
A. The relativistic flying mirror in the nonlinear wake waves	17
VI. Experimental Demonstration of a Relativistic Flying Mirror	19
VII. Extremely High Field Limits	19
Acknowledgment	21
References	21

I. INTRODUCTION

Sources of electromagnetic radiation with wavelengths in the range from microwave to X-ray and gamma-ray are required for a wide variety of problems in fundamental and applied physics.

One of the approaches to realize compact sources of hard electromagnetic radiation with controllable parameters is based on the relativistic mirror concept. Within the framework of this concept an electromagnetic wave reflected from a counter-propagating relativistic mirror is compressed in the longitudinal direction and its carrier frequency is upshifted [1] (see also the review [2] and the literature cited therein).

The question on realization of relativistic mirrors under laboratory conditions has been raised repeatedly over a number of years. In this regard emerges a question on whether or not it is possible to prepare the relativistic mirror of high enough quality for efficient reflection of the light, which can move with substantially large velocity for providing significantly high frequency increase up to the level corresponding to the photon energy in the X-ray range. The answer can be found using the knowledge in the physics of nonlinear processes in relativistic laser plasmas.

One of the ways towards achieving the higher frequency and intensity is based on the simultaneous laser frequency upshifting and pulse compression. It was demonstrated within the relativistic flying mirror (RFM) concept, which uses the laser pulse compression, frequency up-shift, and focusing by counter-propagating thin electron shells [2, 3]. The results of corresponding proof-of-principle experiments are presented in Refs. [4–6] and in Section VI below.

The RFM concept requires substantially high intensity laser radiation interaction with matter. Recent progress in laser technology has lead to a dramatic increase of laser power and intensity, opening new fields of regimes of laser-matter interaction [7–11]. At intensities greater than $10^{18}\text{W}/\text{cm}^2$, the electron quiver energy exceeds its rest mass energy. Under these conditions the laser matter interaction can be described by the electrodynamics of continuous media. In the near future the radiation of ultrashort pulse high power lasers may reach the intensity of $10^{24}\text{W}/\text{cm}^2$ and higher [12]. In this limit protons also become relativistic, while the electron motion becomes strongly dissipative due to its intense hard radiation emission, so that the interaction should be described within the framework of quantum electrodynamics (QED).

In the relativistic regime of the interaction of a high intensity electromagnetic wave with plasmas the nonlinear character of this interaction results in the formation of electron density modulations, including dense electron bunches and/or thin electron layers moving with relativistic velocity. An interaction of the same or another electromagnetic wave with these relativistic objects can be reduced to the wave reflection from relativistic mirrors, which is accompanied by the relativistic frequency shift and change of the reflected wave amplitude. This is the mechanism of the wave intensification and frequency upshifting, including high order harmonics generation, in relativistic collisionless plasma. This underlies the relativistic oscillating mirror concept [13] and the generation of electromagnetic attosecond pulses [14, 15]. The robustness of this mechanism allowed the experimental demonstration of attosecond phase locking of harmonics emitted from laser produced plasmas [16]. The light frequency up-shifting and intensification have been discussed in the problem of a laser interaction with solid density targets, which revealed attosecond pulse and high order harmonics generation [14, 15, 17, 18].

We notice a principal difference between two physical situations. One is the electromagnetic wave scattering by a single relativistic electron, which corresponds to Thomson or, in the quantum limit, to Compton scattering. Another is the wave reflection by a dense enough electron layer moving with relativistic velocity. In both cases the maximum frequency upshift is the same being proportional to the square of the electron's Lorentz factor. However, the number of the emitted photons differs. While in the first case the scattered light intensity is linearly proportional to the number of electrons, in the second case the reflected light intensity is quadratically proportional to that number. In addition, in the first case the scattered radiation is incoherent, and in the second case the reflected light is coherent.

These properties are of paramount importance for developing electromagnetic radiation sources capable of providing the wave intensity approaching the quantum electrodynamics limits [3].

Nowadays there is a demand to understand the cooperative behavior of relativistic quantum systems. It was understood that the vacuum probing becomes possible by using high power lasers [7–10]. With the achievable laser intensity increasing at future facilities [12], we shall encounter novel physical processes such as the radiation reaction dominated regimes and then QED processes. In a micron focal spot, the laser light can generate electron-positron pairs from vacuum at intensity two orders of magnitude below [19] the threshold corresponding to the QED critical electric field, $10^{29}\text{W}/\text{cm}^2$, [20–23]. In this case vacuum begins to act nonlinearly, its refractive index becomes nonlinearly dependent on the electromagnetic field strength [24]. In quantum field theory, particle creation from vacuum has attracted a great deal of attention, because it provides a typical example of non-perturbative processes [23, 25] in quantum field theory.

Relativistic flying mirrors formed by the laser-driven plasma waves can be used [2] to achieve an electromagnetic wave intensification towards reaching the critical field of QED. Nonlinear QED vacuum properties can be probed in the future with such strong and powerful electromagnetic pulses.

As regards to other applications, the electromagnetic field intensification and the frequency upshift are attractive

for research on the development of sources of radiation with tunable parameters. The ultimate goal of these studies is the development of a compact source of high-intensity X-ray radiation, which is required by a broad range of applications, from molecular imaging [26], which is of high interest for medicine and biology, to the diagnostics of thermonuclear plasmas and experiments on laboratory astrophysics [11, 27–29]. We note here the interest towards accelerated relativistic mirrors (see Refs. [30–32]) in the context of studying at the terrestrial laboratory conditions the Unruh and Hawking effects [33].

The present review article focuses on the analytical theory of nonlinear interactions of intense electromagnetic waves with relativistic plasmas related to the RFM concept. The experimental results demonstrating the RFM concept in the high intensity laser interaction with plasmas and corresponding computer simulations can be found in the review articles [2, 7, 8, 11, 17] and in the literature cited therein.

II. RELATIVISTIC FLYING MIRROR CONCEPT FOR ELECTROMAGNETIC FIELD INTENSIFICATION AND FREQUENCY UPSHIFTING

A. Reflection of Electromagnetic Wave from Relativistic Mirror Moving with the Constant Velocity

Change of the frequency and amplitude of an electromagnetic wave reflected by moving mirror occurs due to the double Doppler effect. The corresponding theory of the light reflection from the mirror moving in vacuum with arbitrary (subluminal) velocity was formulated by A. Einstein in his paper on the special theory of relativity [1]. It presents a classical example of the application of the Lorentz transformation formalism for solving the problems of classical electrodynamics. The consideration of photon interaction with relativistic mirrors is of great interest to quantum field theory too [30, 31].

The process of the electromagnetic wave reflection from a relativistic mirror is characterized by several remarkable features. The reflected wave frequency depends on the incidence angle and the mirror velocity. We consider reflection and refraction of the plane monochromatic wave with the frequency ω_0 and wave vector \mathbf{k}_0 due to the plasma slab with the electron density $n_{e,2}$ moving with the velocity $c\beta_M$ along the x -axis, as illustrated in Fig. 1.

In the boosted frame of reference, \mathcal{M} , where the mirror is at rest (Fig. 1 b), the wave reflection and refraction are described by Snell's law, i. e. the incidence and reflection angles are equal to each other, $\theta'_i = \theta'_r$, and the refraction angle is given by equation $\sin \theta'_t / \sin \theta'_i = n'_1 / n'_2$, where n'_1 and n'_2 are the refraction indices in media 1 and 2.

Assuming that media 1 and 2 are plasma regions with the electron density $n'_{e,1}$ and $n'_{e,2}$, respectively, we obtain

$$\sin \theta'_t = \sin \theta'_i \sqrt{\frac{1 - (\omega_{pe,1}/\omega')^2}{1 - (\omega_{pe,2}/\omega')^2}}, \quad (1)$$

where ω' is the wave frequency in the boosted frame of reference and $\omega_{pe,1,2} = \sqrt{4\pi n_{e,(1,2)} e^2 / m_e}$. In this frame of reference the wave frequency and the wave number are given by

$$\omega' = \gamma_M(\omega_0 + k_{0,x}\beta_M c), \quad k'_x = \gamma_M(k_{0,x} + \omega_0\beta_M/c), \quad k'_y = k_{0,y}, \quad (2)$$

with $\gamma_M = 1/\sqrt{1 - \beta_M^2}$ being the mirror relativistic Lorentz factor. As a result of the wave reflection the x component of the wave vector changes sign (Fig. 1 b). By performing the Lorentz transformation to the laboratory frame of reference, \mathcal{L} , we can find the frequency and wave vector of the reflected wave. Taking into account that $\sin \theta_i = k_{0,y}/k_0$, $\sin \theta_r = k_{0,y}/k_r$ and using relationships (2), we obtain

$$\omega_r = \frac{\omega_0(1 + \beta_M^2) + 2\beta_M \sqrt{\omega_0^2 - \omega_{pe,1}^2} \cos \theta_i}{1 - \beta_M^2}. \quad (3)$$

Here ω_0 and ω_r are the frequencies of the incident and reflected waves, respectively. The reflection angle θ_r is related to the wave incidence angle θ_i as

$$\sin \theta_r = \frac{\omega_0}{\omega_r} \sin \theta_i = \frac{\omega_0(1 - \beta_M^2) \sin \theta_i}{\omega_0(1 + \beta_M^2) + 2\beta_M \sqrt{\omega_0^2 - \omega_{pe,1}^2} \cos \theta_i}. \quad (4)$$

If the reflection coefficient is equal to unity, as for the ideally reflecting mirror, then during the wave-mirror interaction the ratio of the amplitude of the electric field to its frequency is constant:

$$\frac{E_r}{\omega_r} = \frac{E_0}{\omega_0}. \quad (5)$$

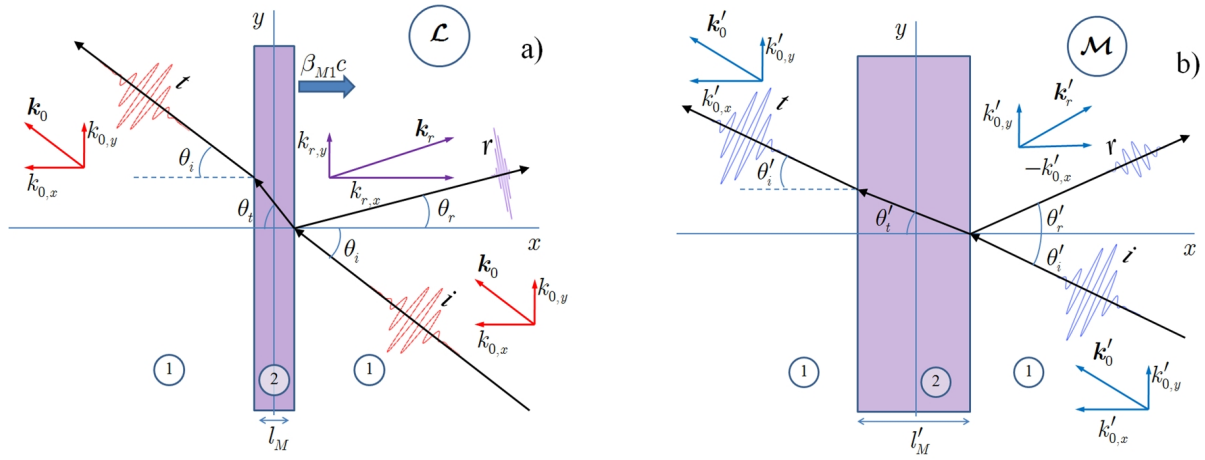


FIG. 1: a) Reflection and refraction of the electromagnetic wave at a plasma slab moving with the velocity $c\beta_M$ along the x -axis. 1 and 2 denote plasma regions with the density equal to n_1 and n_2 , respectively. Incident, reflected, and transmitted waves in a) the laboratory frame of reference \mathcal{L} ; b) the mirror rest frame of reference, \mathcal{M} .

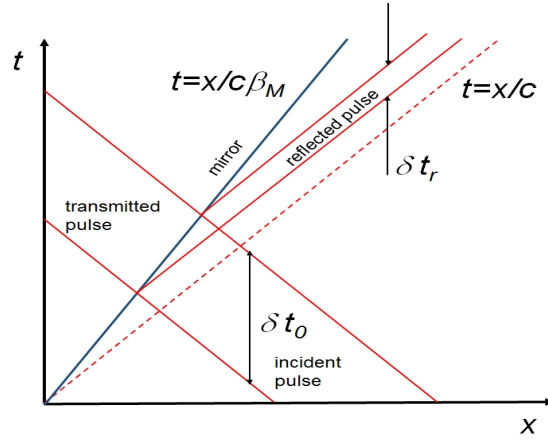


FIG. 2: Reflection of an electromagnetic wave at a semi-transparent relativistic mirror. The mirror moves with a constant velocity $c\beta_M$. The world lines corresponding to the light pulses in vacuum are given by $t = \pm x/c + \text{constant}$.

Depending on whether the wave and mirror are co-propagating ($\beta_M < 0$) or counter-propagating ($\beta_M > 0$) in the laboratory frame of reference we have either the frequency downshift or the upshift, the stretching or the compression of the electromagnetic pulse, and decreasing or increasing of the wave amplitude. In the most simple configuration of the wave propagating in vacuum (i.e. $\omega_{pe,1} = 0$) normally incident on the mirror ($\theta_i = 0$), expression (3) yields

$$\omega_r = \omega_0 \frac{1 + \beta_M}{1 - \beta_M} \equiv \omega_0 (1 + \beta_M)^2 \gamma_M^2. \quad (6)$$

In the ultrarelativistic limit, when $\gamma_M \gg 1$, the reflected wave frequency is higher (lower) by a factor $\approx 4\gamma_M^2$. The reflected wave amplitude changes accordingly.

The results obtained can be qualitatively (and quantitatively) explained by considering the light pulse kinematics illustrated by the simple picture in Fig. 2. It shows in the plane (t, x) the light reflection at the relativistic mirror. The mirror position is given by the line $t = x/\beta_M c$. The world lines corresponding to the incident, reflected and transmitted light pulses are straight lines given by $t = \pm x/c + \text{constant}$. With the help of elementary geometry we find that the width of the reflected pulse δt_r is related to the incident pulse width δt_0 as $\delta t_r = \delta t_0 (1 - \beta_M)/(1 + \beta_M)$ in accordance with expression (6).

B. Light Reflection at the Receding Mirror and Ion acceleration by the Radiation Pressure

The light interaction with a co-propagating plasma slab corresponds to the reflection off a receding mirror. It results in the frequency down-shift and the energy decrease of the reflected radiation. The frequency decreases by a factor $(1 + \beta_M)/(1 - \beta_M)$, Eq. (6), which in the limit $\beta_M \rightarrow 1$ approximately equals $4\gamma_M^2$. The energy of the reflected electromagnetic pulse becomes equal to $\mathcal{E}_{las}(1 - \beta_M)/(1 + \beta_M)$, where \mathcal{E}_{las} is the energy of the laser pulse incident on the mirror. As a result, the energy transferred to the target is given by $2\mathcal{E}_{las}\beta_M/(1 + \beta_M)$. This process corresponds to the ion acceleration by the radiation pressure of the laser light [34–36]. As we see, in the limit $\gamma_M \gg 1$ almost all the energy of the laser pulse is transferred to the accelerated ions [35].

In general case, the energy of the accelerated ions \mathcal{E}_p (here we assume that the ions are protons) is determined by the laser energy \mathcal{E}_{las} and by the total number of the ions in the region of target irradiated by the laser pulse, \mathcal{N}_{tot} :

$$\mathcal{N}_{tot}\mathcal{E}_p = 2\mathcal{E}_{las}\frac{\beta_M}{1 + \beta_M}. \quad (7)$$

In the non-relativistic ion energy limit we obtain the scaling: $\mathcal{E}_p = 400 \times (10^{11}/\mathcal{N}_{tot})^2(\mathcal{E}_{las}/10 \text{ J})^2 \text{ MeV}$.

There are first indications of the ion acceleration by laser radiation pressure obtained in experiments on the laser interaction with thin foil targets [37–39].

In the case of the incident/reflected light pulse propagating in a continuous medium, the light reflection at the moving mirror acquires other properties including the parametric Doppler effect and the effects of finite group velocity of the electromagnetic pulse (e.g. see review article [2] and the literature cited therein). This, in particular, becomes important in the case of the ion acceleration by the radiation pressure [35] of “slow” light [40–42], which may be of special interest in the so called double-sided relativistic mirror configuration [43]. The changing group velocity medium through which the incident laser pulse propagates can be a preplasma corona formed due to the finite contrast of the laser pulse as discussed in Ref. [44].

If medium, through which the wave propagates, moves one should also take into account the Fizeau effect – the light dragging along by the medium [45]. According to definition of the group velocity of the electromagnetic wave, $\mathbf{v}_g = \partial_{\mathbf{k}}\omega$, we have the relationships

$$d\omega = \mathbf{v}_g \cdot d\mathbf{k}, \quad d\omega' = \mathbf{v}'_g \cdot d\mathbf{k}' \quad (8)$$

in the laboratory and boosted frames of references. We find

$$d\omega = \gamma_M(d\omega' + c\beta_M dk'_x) = \gamma_M(\mathbf{v}'_g \cdot d\mathbf{k}' + c\beta_M dk'_x) \quad (9)$$

and

$$\gamma_M \left(1 + \frac{\beta_M}{c} v'_{g,x}\right) d\omega = \gamma_M(v'_{g,x} + c\beta_M) dk'_x + v'_{g,y} dk'_y + v'_{g,z} dk'_z, \quad (10)$$

which yields

$$v_{g,x} = \gamma_M \frac{v'_{g,x} - c\beta_M}{1 - \frac{v'_{g,x}\beta_M}{c}}, \quad v_{g,y} = \gamma_M \frac{v'_{g,y}}{1 - \frac{v'_{g,x}\beta_M}{c}}, \quad v_{g,z} = \gamma_M \frac{v'_{g,z}}{1 - \frac{v'_{g,x}\beta_M}{c}}. \quad (11)$$

In the case of the wave interacting with the receding mirror, i. e. in the co-propagating configuration, we notice that the wave group velocity should not be lower than the mirror velocity [46],

$$v_g = c \frac{\sqrt{\omega_0^2 - \omega_{pe}^2}}{\omega_0} \geq c\beta_M. \quad (12)$$

This is equivalent to the constraint $\omega_0 \geq \omega_{pe}\gamma_M$. If the mirror moves faster than the laser group velocity, the laser pulse cannot accelerate it. This imposes an upper limit on the energy of accelerated ions [40–42].

C. Light Reflection at the Accelerated Mirror

We consider the wave reflection from the accelerated mirror for the case of normal incidence [30, 31]. The incident and reflected electromagnetic waves in vacuum obey Maxwell’s equations from which follows the wave equation for transverse component of the vector potential,

$$\partial_{tt}A - c^2\partial_{xx}A = 0. \quad (13)$$

The mirror coordinate at time t is determined by equation $\mathcal{M}(x, t) = \text{const}$, so that the mirror is located in the point $x = x_M(t)$, Fig. 3 a).

We assume that the boundary condition for the field at the mirror is reduced to the Dirichlet condition

$$A(x, t)|_{x=x_M(t)} = 0. \quad (14)$$

This boundary condition is given at the non-stationary surface. Following Ref. [31], we change the independent variables (t, x) to new variables (τ, ξ) , for which the mirror is at the rest and the equation (13) remains the wave equation for $A(\xi, \tau)$.

At first, it is convenient to introduce the advanced and retarded coordinates (u, v) :

$$u = t - x/c \quad \text{and} \quad v = t + x/c. \quad (15)$$

In these coordinates Eq. (13) takes the form

$$\partial_{uv}A = 0. \quad (16)$$

In coordinates (\bar{u}, \bar{v}) , determined by $u = f(\bar{u})$ and $v = g(\bar{v})$, equation (16) preserves its form except for a factor $f'g'$: $\partial_{\bar{u}\bar{v}}A = 0$.

In new spatial and time coordinates, (ξ, τ) , defined as

$$\bar{u} = \tau - \xi/c \quad \text{and} \quad \bar{v} = \tau + \xi/c, \quad (17)$$

equation (13) is

$$\partial_{\tau\tau}A - c^2\partial_{\xi\xi}A = 0. \quad (18)$$

We choose the functions $f(\tau - \xi/c)$ and $g(\tau + \xi/c)$ to be such that the mirror is at rest at $\xi = 0$, which implies the equation for the functions f and g ,

$$g(\tau) - f(\tau) = 2x_M((g(\tau) + f(\tau))/2), \quad (19)$$

transforming the boundary condition (14) to

$$A(\xi, \tau)|_{\xi=0} = 0. \quad (20)$$

We may choose the function $g(\bar{v})$ to be equal to $g(\bar{v}) = \bar{v}$. This leads to the functional equation for f :

$$\tau - f(\tau) = 2x_M((\tau + f(\tau))/2), \quad (21)$$

Solution to the boundary problem for Eq. (18) with the boundary condition (20) is

$$A(\xi, \tau) = A_0 \exp(\pm i\omega_0\tau) \sin \omega_0\xi. \quad (22)$$

In the coordinates (t, x) it can be written as

$$A(x, t) = A_0 [\exp(-i\omega_0v) - \exp(i\psi_r(u))]. \quad (23)$$

Here variables u and v are defined by Eq. (15) and the function $\psi_r(u)$ is the phase of the reflected wave (the ratio $\psi_r(u)/\omega_0$ is the inverse function to $f(u)$). Using Eq. (21) we obtain that the phase, $\psi_r(u)$, is given by

$$\psi_r(u) = \int^u \omega_r(u) du = \omega_0[2t(u) - u], \quad (24)$$

where we have introduced the frequency of the reflected wave $\omega_r(u)$ related to the phase $\psi_r(u)$. Here $t(u)$ should be found from the equation

$$t(u) = u + x_M(t(u))/c, \quad (25)$$

in other words, it can be obtained by finding the position of the light ray intersection with the world line of the mirror in the (t, x) plane. Here $x_M(t(u))$ is the intersection point coordinate, see Fig. 3 a).

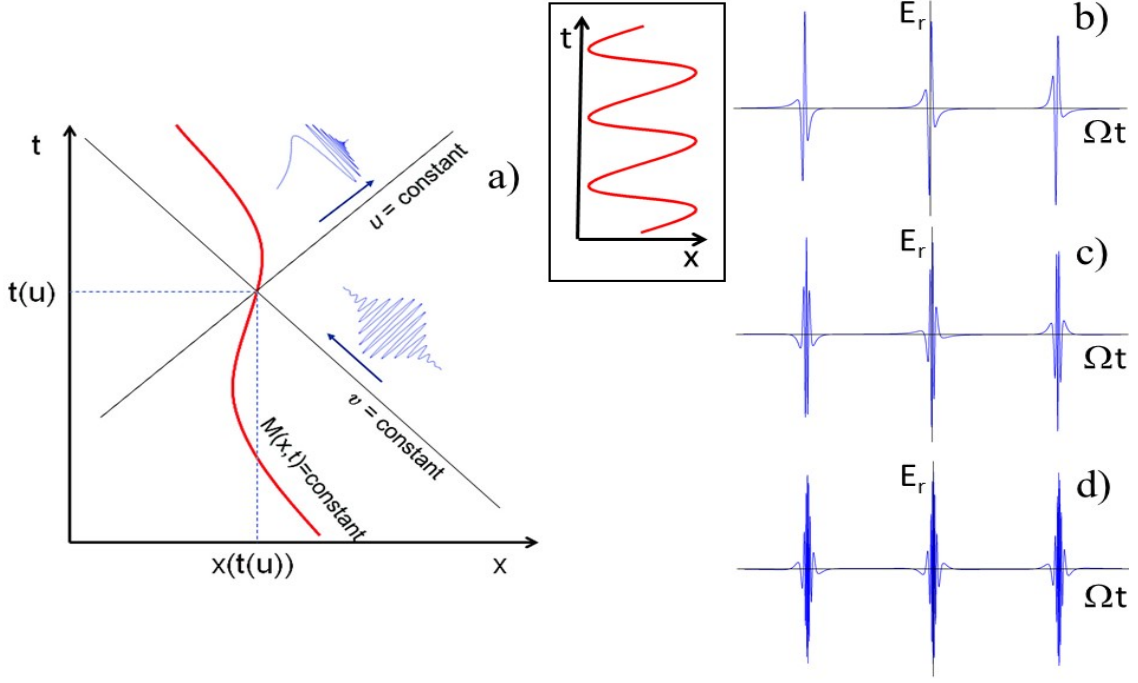


FIG. 3: a) The mirror world line in the (t, x) plane. The incident, $v = \text{constant}$, and reflected, $u = \text{constant}$, light rays. b), c), d) The electric field of the wave reflected from the oscillating mirror for $a_0 = 15$ and $\Omega/\omega_0 = 0.5, 1, 2$, respectively.

Differentiating the expression for the phase $\psi_r(u)$ with respect to time, we find

$$\psi_r'(u) = \omega_0 \frac{1 + \beta_M(u)}{1 - \beta_M(u)}, \quad (26)$$

where $\beta_M(u) = dx_M(t(u))/cdt$ is the mirror velocity normalized by c . The derivative of the phase with respect to variable u determined by Eq. (24) is nothing more than the frequency of the reflected wave, ω_r .

When the mirror moves with uniform acceleration, w_M , a dependence of its coordinate on time is given by the relationship [45]

$$x_M(t) = \frac{c}{w_M} \sqrt{c^2 + w_M^2 t^2}. \quad (27)$$

In this case the frequency of light reflected from the uniformly accelerated mirror in the limit $t \rightarrow \infty$ grows proportionally to the square of the time for positive acceleration, $w_M > 0$, and decreases inversely proportional to the square of the time for negative acceleration $w_M < 0$:

$$\omega_r = \omega_0 \frac{\sqrt{c^2 + w_M^2 t^2} + w_M t}{\sqrt{c^2 + w_M^2 t^2} - w_M t} \underset{t \rightarrow \infty}{\approx} \begin{cases} 4\omega_0 w_M^2 t^2 / c^2, & w_M > 0 \\ \omega_0 c^2 / 4w_M^2 t^2, & w_M < 0 \end{cases} \quad (28)$$

The amplitude of the reflected wave increases (decreases) in a similar way.

III. THIN ELECTRON LAYER AS A RELATIVISTIC MIRROR

The interaction of a sufficiently wide electromagnetic pulse with a thin foil, in the case where the ponderomotive force of the pulse significantly exceeds the force caused by the electric field, which occurs due to electric charge separation, can result in the formation of a dense electron layer moving in the direction of electromagnetic wave propagation. The second counter-propagating electromagnetic pulse is partially reflected from a thin electron layer,

which, due to the above-mentioned double Doppler effect, should lead to the compression of the reflected pulse and to its frequency upshift [47]. This scheme has attracted recently significant attention both in theoretical work [48–52] and in experiment [53].

As a simple model of the acceleration of a thin electron layer by a laser pulse, we use the known exact solution of the equations of motion of a charged particle in the field of a plane electromagnetic wave [45]. For the velocity of the electron layer motion along the x -axis it yields

$$v_{\parallel} = \frac{p_{\parallel}}{m_e \gamma_e} = c \frac{|\mathbf{a}_{\perp}(u)|^2}{2 + |\mathbf{a}_{\perp}(u)|^2} \quad (29)$$

with $u = t - x/c$. The layer coordinate is defined by implicit equations given in Ref. [45]. For a circularly polarized wave, for example, with a constant dimensionless amplitude a_0 , we obtain

$$x(t) = \frac{2x_0 + a_0^2 ct}{2 + a_0^2}, \quad (30)$$

where x_0 is the layer coordinate value at the instant of arrival of the laser pulse, $t_0 = x_0/c$.

Using the expression for the electron velocity in Eq. (29), we find the corresponding gamma-factor of the relativistic mirror:

$$\gamma_M(u) = \frac{1}{\sqrt{1 - v_{\parallel}^2(u)/c^2}} = \frac{2 + |\mathbf{a}_{\perp}(u)|^2}{2\sqrt{1 + |\mathbf{a}_{\perp}(u)|^2}}, \quad (31)$$

It can be seen that in the limit of a large-amplitude electromagnetic wave, when $|\mathbf{a}_{\perp}(u)| \gg 1$, the gamma-factor is proportional to the first power of $|\mathbf{a}_{\perp}(u)|$.

A. Light Reflection at the Oscillating Mirror

When an electromagnetic wave reflects from an oscillating mirror, its frequency spectrum extends to the high frequency range and the wave breaks up to short wave packets, as shown in Fig. 3 b), c), and d). According to Eq. (3) the wave frequency increases by a factor approximately equal to $4\gamma_M^2$. By the same factor the maximal electric field increases according to Eq. (5).

The relativistic oscillation mirror (ROM) concept has been proposed in Ref. [13] as a mechanism of high order harmonic generation when an overdense plasma is irradiated by relativistically intense laser radiation. High frequency radiation generation has been demonstrated in experiments with multi-terawatt lasers, see review article [17], literature cited therein and discussions of alternative mechanisms.

As an illustration of this process we consider a thin electron layer oscillating under the action of a linearly polarized electromagnetic wave of the frequency Ω . The wave's electric field is parallel to the y axis: $E_y = E_0 \cos(\Omega v)$ with $v = t + x/c$. The second electromagnetic wave with the amplitude a_i is reflected from the electron layer as from the mirror. In order to describe the electron layer motion we use here the results of an exact solution of the problem on the electric charge dynamics in the field of an electromagnetic wave [45], which yield the parametric dependences of the charge coordinates and momentum components on time in the frame of reference where the charge is on average at the rest:

$$x = \frac{a_0^2}{4(2 + a_0^2)} \sin 2\eta, \quad y = \frac{a_0}{\sqrt{1 + a_0^2/2}} \cos \eta, \quad z = 0, \quad (32)$$

$$t = \eta + \frac{a_0^2}{4(2 + a_0^2)} \sin 2\eta, \quad (33)$$

$$p_x = \frac{a_0^2}{4\sqrt{1 + a_0^2/2}} \cos 2\eta, \quad p_y = a_0 \sin \eta, \quad p_z = 0. \quad (34)$$

Here the coordinates and time are normalized by c/Ω and Ω^{-1} , respectively, $\eta = \Omega v$, the momentum is measured in units of $m_e c$, the normalized amplitude of the wave equals $a_0 = eE_0/m_e \Omega c$. The incident wave has a constant amplitude.

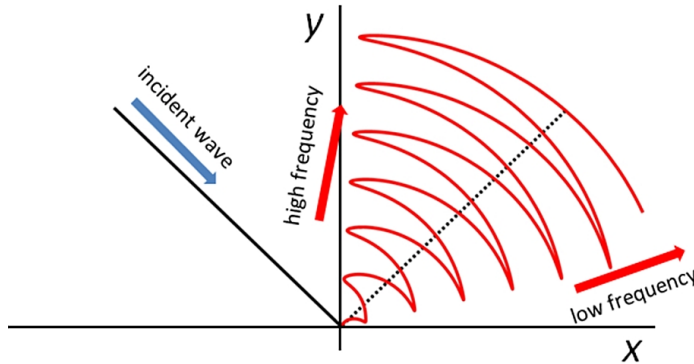


FIG. 4: The instantaneous distribution of photons reflected by an oscillating mirror in the (x, y) plane, for an obliquely incident wave. The photons with the upshifted frequency propagate closer to the mirror normal direction, while low frequency photons are emitted at a grazing angle with respect to the mirror plane.

Now we can calculate the phase and frequency of the reflected wave and find the electric field

$$E_r(t) = E_i \omega_0^{-1} \psi'_r(t) \cos \psi_r(t). \quad (35)$$

This is shown in Figs. 3 b), c), and d) for $\Omega = \omega_0/2$, $\Omega = \omega_0$, and $\Omega = 2\omega_0$, respectively, where the mirror oscillation amplitude is characterized by $a_0 = 15$. The reflected radiation has the form of a sequence of wave packets with the frequency in the limit $a_0 \gg 1$ approximately equal to $\omega_0 a_0^2/2$ and with the wave packet duration $\approx 2\pi/\Omega a_0$. Here we assume that the second wave propagates in the direction opposite to that of the wave which drives the mirror oscillations. If the second wave and the wave driving the mirror oscillations propagate in the same direction then the electric field in the reflected wave has a form of a sequence of short pulses with the width $\approx \pi/\Omega a_0$ with no high frequency filling. We note that the generation of ultrashort electromagnetic pulses observed in computer simulations of the relativistically strong electromagnetic wave interaction with an overdense plasma target in Ref. [15] has been explained by the authors within the framework of the ROM concept.

According to Eq. (4) the angle of light reflection θ_r depends on the mirror velocity. The larger the mirror positive velocity the closer the reflected light propagation direction is to the mirror normal. For photons reflected in the mirror negative velocity phase, the propagation direction is close to the mirror surface. The photons with the upshifted frequency are localized in the region close to the mirror normal direction. The low frequency photons propagate at a grazing angle with respect to the mirror plane. Using expressions (32, 33, 34) we can find the instantaneous photon distribution in the (x, y) plane for the electromagnetic wave reflected by oscillating mirror which is shown in Fig. 4. This can be considered as a lighthouse effect. The attosecond lighthouses from oscillating plasma mirrors have been demonstrated in Ref. [54], where an isolated nonlinearly generated attosecond pulse train has been obtained by rotating the instantaneous wavefront direction of an intense few-cycle laser field. Here we show that the angle separation of high and low frequency photons can also occur due to the relativistic dependence of the reflection angle on the instantaneous velocity of the oscillating mirror.

B. Reflection Coefficient of Electromagnetic Radiation from a Thin Electron Layer

Here we discuss the reflection of electromagnetic waves from a thin electron layer. In order to calculate the coefficients of reflection, \mathbf{R} , and transmission, \mathbf{T} , we consider the interaction of electromagnetic waves with a strongly nonuniform electron distribution. The electrons reside in a layer with the density n , which determines the plasma frequency as a function of coordinate and time,

$$\omega_{pe} = \sqrt{\frac{4\pi n(x - c\beta_M t)e^2}{m_e \gamma_M}}. \quad (36)$$

Performing the Lorentz transformation to a boosted frame reference moving with the velocity $c\beta_M$, we find that in this frame of reference, the wave equation describing the electromagnetic wave interaction with the plasma slab takes

the form

$$\frac{d^2 a(\zeta)}{d\zeta^2} + q^2(\zeta)a(\zeta) = 0, \quad (37)$$

where

$$q^2(\zeta) = s^2 + \nu_e(\zeta). \quad (38)$$

Here $\nu_e(\zeta) = \omega_{pe}^2/c^2$, and variables

$$s^2 = (\omega'/c)^2 - k_y^2, \quad \zeta = \gamma_M(x - c\beta_M t), \quad t', \quad k' \quad \text{and} \quad \omega' \quad (39)$$

are the square of the wave number, coordinate, time, incident wave number and frequency in the boosted frame of reference, respectively. The vector potential is normalized by $m_e c^2/e$, and its dependence on time t' and coordinates ζ and y is

$$a(\zeta) = \frac{eA_z(\zeta)}{m_e c^2} \exp[-i(\omega' t' - k_y y)]. \quad (40)$$

The reflection coefficient of electromagnetic radiation from a thin electron layer we find in a similar way as is done in the classical problem of scattering. Assuming that the layer is in the rest frame of reference, we take the distribution of the electron density in the form proportional to the Dirac delta function: $n(\zeta) = n_0 l_0 \delta(\zeta)$, where l_0 is the electron layer thickness.

In this case the function $\nu_e(\zeta)$ in Eq. (38) is $\nu_e = g_\delta \delta(\zeta)$ with $g_\delta = k_p^2 l_0$ and $k_p = \omega_{pe}/c$. Integrating this equation over ζ in the interval $-\varepsilon < \zeta < \varepsilon$ and letting ε go to zero, we obtain the condition for the jump of the derivative $da/d\zeta$ on the boundary $\zeta = 0$:

$$\left. \frac{da}{d\zeta} \right|_{+0} - \left. \frac{da}{d\zeta} \right|_{-0} = g_\delta a(0). \quad (41)$$

The function $a(\zeta)$ is continuous in the point $\zeta = 0$. The solution to Eq. (37), describing the wave reflection from a thin layer can be represented as

$$a(\zeta) = \begin{cases} \exp(is\zeta) + \rho \exp(-is\zeta), & \zeta \geq 0, \\ \tau \exp(is\zeta), & \zeta \leq 0, \end{cases} \quad (42)$$

where ρ and τ are related to each other by the equations following from the boundary condition (41):

$$1 + \rho(s) = \tau(s), \quad (43)$$

$$iq[1 - \rho(s) - \tau(s)] = g_\delta \tau(s). \quad (44)$$

As a result the reflected wave amplitude is equal to

$$\rho(s) = -\frac{g_\delta}{2is + g_\delta}. \quad (45)$$

From this expression we obtain the reflection coefficient for the number of photons

$$\mathbf{R}_\delta = \frac{g_\delta^2}{4s^2 + g_\delta^2}. \quad (46)$$

For large values of the electron surface density, $n_0 l_0$, i. e. for $g_\delta^2 \gg 4s^2$, the reflection coefficient is close to unity. In the opposite limit, we can neglect g_δ^2 as compared with $4s^2$ in the denominator of the right-hand side of the expression (46) and obtain

$$\mathbf{R}_\delta \approx \frac{g_\delta^2}{4s^2} \approx \frac{\varepsilon_e^2}{\gamma_M^2}. \quad (47)$$

where the dimensionless parameter introduced in Ref. [55]

$$\varepsilon_e = n_0 l_0 \lambda_0 r_e = \frac{2\pi n_e l}{m_e \omega_0 c} \quad (48)$$

characterizes the relativistic transparency of a thin foil target. It is seen that the reflection coefficient is proportional to the square of the electron density in the surface layer, $n_0 l_0$, i. e. the reflection is coherent.

In the thin electron layer paradigm of a relativistic mirror, the effects of Coulomb explosion and transverse modulations caused by the electromagnetic pulse non-uniformity can deteriorate the property of the reflected radiation. As shown in Ref. [49], sufficiently homogeneous laser pulses are required to form thin electron layers continuous in the transverse direction. When this condition is not fulfilled in the interaction of laser radiation with a thin foil, a cloud of ultrashort bunched electrons (a swarm of electron bunches) is formed, resulting in loss of coherency and broadening of the reflected pulse frequency spectrum. Contrary to that the relativistic flying mirror concept using the wake plasma wave (considered below) shows more stable and robust behavior.

C. Relativistic Transparency of a Thin Plasma Layer

The 1D electrodynamics model, where the role of a point charge is played by an infinitely thin foil [55–57], has been extensively used in studying the problem of relativistic thin plasma layer transparency, particularly for the purposes of the laser pulse shaping [55] (see also the experimental paper [58]), in high order harmonics generation [59–61], in laser ion acceleration [61], in the analysis of the radiation friction effects [62] and in the generation of coherent extremely high intensity x-ray pulses by relativistic mirrors [3, 47].

Using the results of Refs. [55, 56, 61], we consider the case of normal incidence of a plane electromagnetic wave on an infinitely thin foil. The foil is located in the plane $x = 0$. The interaction of the wave with the foil is described by Maxwell's equations for the vector potential $\mathbf{A}(x, t)$ which yield

$$\partial_{tt} \mathbf{A} - c^2 \partial_{xx} \mathbf{A} = 4\pi c \delta(x) \mathbf{J}(\mathbf{A}). \quad (49)$$

The term on the r.h.s. describes the electric current in the foil and the delta-function represents its sharp localization. The solution to the initial problem for Eq. (49) yields

$$\mathbf{A}(x, t) = \mathbf{A}_0(x, t) + 2\pi \int_0^{t-|x|/c} \mathbf{J}(\mathbf{A}(0, \tau)) d\tau, \quad (50)$$

where $\mathbf{A}_0(x, t)$ is a known function describing the incident electromagnetic wave. Assuming $x = 0$ on both sides of Eq. (50) and taking the derivative with respect to time, we obtain

$$\frac{d\mathbf{A}(0, t)}{dt} = \frac{d\mathbf{A}_0(0, t)}{dt} + 2\pi \mathbf{J}(\mathbf{A}(0, t)). \quad (51)$$

In this way a nonlinear boundary problem for a system of partial differential equations is reduced to the ordinary differential equation for the field inside the foil, $\mathbf{A}(0, t)$.

In the case of the circularly polarized electromagnetic wave, it is convenient to write the longitudinal and transverse components of electron momentum, p_x and $p_y \mathbf{e}_y + p_z \mathbf{e}_z$, as a combination of vectors, having components rotating with angular frequency ω ,

$$\begin{pmatrix} p_1 \\ p_2 \\ p_3 \end{pmatrix} = \begin{pmatrix} 1 & 0 & 0 \\ 0 & \sin \omega t & -\cos \omega t \\ 0 & \cos \omega t & \sin \omega t \end{pmatrix} \begin{pmatrix} p_x \\ p_y \\ p_z \end{pmatrix} \quad (52)$$

where p_2 and p_3 are the components parallel and perpendicular to the electric field. Taking into account the generalized electron momentum conservation, $\mathbf{p} - e\mathbf{A}/c = \text{constant}$, and the relationship between the electric current and the electron velocity, $\mathbf{J} = -en_e l \mathbf{v} = -en_e l c \mathbf{p} / (m_e c^2 + p^2)^{1/2}$, where n_e and l are the electron density and the foil thickness, respectively, we find that the 1D equation (51) for the stationary motion of a thin foil interacting with a rotating electric field can be written in the form

$$p_2 = \varepsilon_e \frac{p_3}{\gamma_e}, \quad (53)$$

$$p_3 = a - \varepsilon_e \frac{p_2}{\gamma_e} \quad (54)$$

where $\gamma_e = \sqrt{1 + p_2^2 + p_3^2}$ and the parameter ε_e is defined by Eq. (48).

Solving this system of algebraic equations we obtain

$$p_2 = \frac{\varepsilon_e}{\sqrt{2a}} \frac{\sqrt{(1 - a^2 + \varepsilon_e^2)^2 + 4a^2} - (1 - a^2 + \varepsilon_e^2)}{\sqrt{(1 - a^2 + \varepsilon_e^2)^2 + 4a^2} + (1 - a^2 + \varepsilon_e^2)}, \quad (55)$$

$$p_3 = \frac{\sqrt{(1 - a^2 + \varepsilon_e^2)^2 + 4a^2} - (1 - a^2 + \varepsilon_e^2)}{2a}. \quad (56)$$

In the limit of a relatively weak electromagnetic field when $1 \ll a \ll \varepsilon_e$ expressions (55) and (56) have the asymptotics

$$p_2 = \frac{\varepsilon_e}{1 + \varepsilon_e^2} a - \frac{\varepsilon_e^2}{(1 + \varepsilon_e^2)^3} a^3 + O(a^5), \quad (57)$$

$$p_3 = \frac{a}{1 + \varepsilon_e^2} - \frac{\varepsilon_e(1 - \varepsilon_e^2)}{(1 + \varepsilon_e^2)^3} a^3 + O(a^5). \quad (58)$$

In the opposite limit for $1 \ll \varepsilon_e^{-1/3} \ll a$ the asymptotics are

$$p_2 = \varepsilon_e - \frac{\varepsilon_e(1 + \varepsilon_e^2)}{2a} + O(a^{-3}), \quad (59)$$

$$p_3 = a - \frac{\varepsilon_e^2}{a} + O(a^{-3}). \quad (60)$$

As we can see, in the range of parameters, which corresponds to a relatively low electromagnetic field amplitude $a \ll \varepsilon_e$, the component of the electron momentum p_3 parallel to the electric field is much larger than the perpendicular component p_2 . In the limit of a strong electric field $a \gg \varepsilon_e$ we have $p_2 \gg p_3$, that is, the electron momentum is almost perpendicular to the instantaneous direction of the electric field.

Using obtained expressions (55) and (56) and equation (50) we can find the amplitudes of the reflected and transmitted waves. If the incident wave has moderate intensity, $a \ll \varepsilon_e$, amplitudes of the reflected and transmitted waves are

$$a_r = \frac{a\varepsilon_e}{\sqrt{1 + \varepsilon_e^2}} \quad \text{and} \quad a_t = \frac{a}{\sqrt{1 + \varepsilon_e^2}}. \quad (61)$$

We see that for $\varepsilon_e \gg 1$ the wave is reflected almost totally, while in the limit $\varepsilon_e \ll 1$ the electron layer is transparent.

For ultrahigh intensity, $a \gg 1$, if $a \gg \varepsilon_e \gg 1$, the amplitude of the reflected wave equals ε_e , while the change in the transmitted wave amplitude, $\sqrt{a^2 - \varepsilon_e^2}$, is small. This regime can be explained by taking into account the fact that the electric current density in a plasma cannot exceed $j_{lim} = enc$ since the electron velocity is limited by the speed of light in vacuum.

We see that the condition for the foil to be transparent to the electromagnetic radiation in the limit of moderate intensity $a \ll 1$ is $\varepsilon_e \ll 1$. It can be rewritten as $\omega \gg \omega_{pe}(\pi l/\lambda_p)$, where $\lambda_p = 2\pi c/\omega_{pe}$, which differs from the transparency condition for uniform plasmas by the factor $\pi l/\lambda_p$.

For relativistically strong waves with $a \gg 1$, a foil with $\varepsilon_e \gg 1$ is transparent if $a \gg \varepsilon_e$. This condition can be cast in the form

$$\omega \gg \frac{\omega_{pe}^2 l}{2ca}, \quad (62)$$

while the transparency condition for a uniform extended plasma irradiated by relativistically strong radiation can be written as

$$\omega \gg \frac{\omega_{pe}}{(1 + a^2)^{1/4}}. \quad (63)$$

The expressions for the reflected and transmitted waves have been obtained in the frame of reference, where the plasma layer is at rest. The parameters of the reflected and transmitted waves in the boosted frame of reference, i.e. the electric field amplitudes, E_r , E_t , and the frequencies, ω_r , ω_t , can be found using Lorentz transformations while taking into account the Lorentz invariance of the normalized amplitudes $a_r \propto E_r/\omega_r$ and $a_t \propto E_t/\omega_t$.

IV. NONLINEAR PLASMA WAVES AS RELATIVISTIC MIRRORS

An approach to generate high frequency radiation based on the concept of the relativistic flying mirror utilizes a plasma shell traveling close to the speed of light and acting as a relativistic mirror. Reflected light undergoes double Doppler frequency up-shift, compression, intensification due to relativistic effects and focusing (if the plasma shell is curved).

Relativistic plasma oscillation waves can be generated in the plasma in various ways. When the laser radiation interacts with an inhomogeneous plasma, e.g. with the plasma corona formed at the front surface of a solid target, Langmuir oscillations are excited in the vicinity of the plasma critical density surface, which is also called the plasma resonance region. These Langmuir oscillations take the form of a localized wave packet whose group velocity is zero while its phase velocity is directed against the gradient of the plasma density [63, 64]. Sufficiently high amplitude oscillations eventually break producing thin dense electron layers, which can play a role of relativistic mirrors for the incident electromagnetic radiation. We note that thin electron layers are also formed during the so-called ‘‘vacuum heating’’ [65] at the plasma vacuum interface. Scattering of the electromagnetic wave at such thin electron layers have been associated in Ref. [13] (see Fig. 7 (d) therein) with high order harmonic generation (see also the recent work [66]).

Another, one of the most widely used methods, involves the use of a relatively short high-intensity laser pulse with a length less than or of the order of the plasma wavelength whose normalized amplitude is large enough. Such a laser pulse, propagating in a collisionless plasma, excites the plasma waves in a wake behind it [67, 68]. Nonlinear wake waves can break forming thin dense electron layers (relativistic plasma mirrors) at the wave crest. Various schemes of the relativistic mirrors were described [2, 3, 32, 69] and experimentally demonstrated [4–6] proving a feasibility of the RFM concept.

A. Plasma Oscillations Excited in Near-Critical Inhomogeneous Plasma

Let us consider an electromagnetic wave obliquely incident on an inhomogeneous plasma forming an angle θ_i with respect to the unperturbed plasma surface. Unperturbed electron density in the vicinity of the critical density surface (resonance surface) can be approximated by a linear function: $n_0(x) = n_0(1 - x/L)$. Here L is the scale length of the plasma inhomogeneity. Due to the resonance condition we have $n_0 = m_e \omega_0^2 / 4\pi e^2$, i.e. the Langmuir frequency locally depends on the coordinate as $\omega_{pe}(x) = \omega_0 \sqrt{1 - x/L}$. In the vicinity of the plasma resonance surface, the field of the p-polarized wave with the electric field in the plane of incidence has a singularity [63]. At the singularity the electric field component parallel to the gradient of the plasma density is given by

$$E_x = \frac{E_d \sin \theta_i}{\varepsilon(x)}, \quad (64)$$

where E_d is the driver field related to the incident wave amplitude as

$$E_d = \frac{E_0}{\sqrt{2\pi\omega_0 L/c}} \phi \left(\left(\frac{\omega_0 L}{c} \right)^{1/3} \sin \theta_i \right) \quad (65)$$

with the maximum $\phi(0.8) \approx 1.2$, and the dielectric constant

$$\varepsilon(x) = 1 - \frac{\omega_{pe}^2(x)}{\omega_0(\omega_0 + i\nu_{eff})} \underset{x \rightarrow 0}{\approx} \frac{x}{L} + is. \quad (66)$$

Here the parameter $s = \nu_{eff}/\omega_0$ with the effective decay rate ν_{eff} describes the effects of small dissipation, weak nonlinearity, dispersion, etc. [64].

The maximum of the x -component of the electric field in the plasma resonance region is about $E_m = E_d/s$. The width of the plasma resonance region is equal to $\Delta x = sL$.

For the sake of simplicity we consider here small amplitude plasma oscillations. For the analysis of nonlinear plasma oscillations in the resonance region see Refs. [64] and [13]. The motion of the electron fluid element in the x direction is described by the equation

$$\ddot{\xi}_x = -eE_x/m_e, \quad (67)$$

where ξ_x is the x -component of the electron displacement. From this equation, using expressions (64) and (66) we obtain for ξ_x

$$\xi_x = r_E \frac{s \sin(\omega_0 t) - (x/L) \cos(\omega_0 t)}{(x/L)^2 + s^2} \quad (68)$$

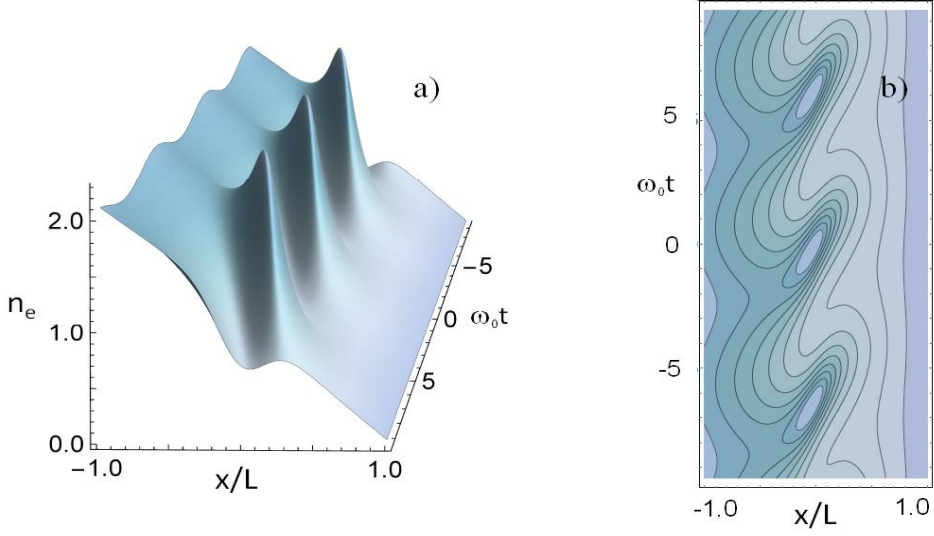


FIG. 5: The electron density modulations in the vicinity of the plasma resonance region given by Eqs. (68) and (70) for $r_E = 0.05$, $s = 0.3$ and $L = 1$. a) n_e vs x and t . b) Constant density contours in the (x, t) plane.

with $r_E = eE_d \sin \theta_i / m_e \omega_0^2$ being the amplitude of the electron quiver motion. As we see Eq. (68) describes the localized Langmuir wave packet of width $\Delta x = sL$ with the plasma oscillations inside having the form of a wave propagating against the density gradient with the phase velocity equal to

$$v_{ph} = \omega_0 \Delta x = s\omega_0 L. \quad (69)$$

This causes the electron density modulations. Using the known dependence of the function ξ_x on time and coordinate we can calculate the electron density. It is given by

$$n_e \approx n_0(x)(1 - \partial_x \xi_x). \quad (70)$$

According to Eqs. (68) and (70) the density modulations have the form of spikes appearing and disappearing in the plasma resonance region as shown in Fig. 5. In other words, we have plasma mirrors periodically appearing and disappearing at the plasma critical surface. The electromagnetic wave reflection at such mirrors results in the generation of a train of ultra-short pulses as illustrated in Fig. 6. Each pulse duration is about $\Delta T = g^{-1}(2\pi/\omega_0)$. The frequency upshifting factor $g = \omega_r/\omega_0$ according to Eq. (6) is $g = \gamma_{ph}^2(1 + \beta_{ph}^2)$. Here $\beta_{ph} = v_{ph}/c$ and $\gamma_{ph} = 1/\sqrt{1 - \beta_{ph}^2}$.

Below we shall see that the electromagnetic wave reflection is maximal for the breaking plasma oscillations. At the wave breaking threshold the electron velocity equals the phase velocity of the wave, i.e. $\gamma_e = \gamma_{ph}$. In the case of plasma oscillations driven by the relativistically intense electromagnetic wave with the normalized amplitude a_0 the electron quiver energy Lorentz factor approximately equals $\gamma_e = a_0$. As a result we have for the frequency upshifting factor $g \approx 2a_0^2$.

We note that the train of almost identical short pulses, produced via reflection off the periodically appearing and disappearing relativistic mirrors, has a spectrum consisting of high-order harmonics. The width of an individual harmonic is inversely proportional to the number of short pulses, which is determined by the duration of the incident electromagnetic wave and by the life-time of the plasma resonance region.

B. Nonlinear Wake Wave Excited by a Short Laser Pulse in Underdense Plasmas

Finite amplitude plasma oscillations excited in an underdense plasma by a short relativistically intense laser pulse can be described using the system of Maxwell's equations and the cold hydrodynamics equations for the electron

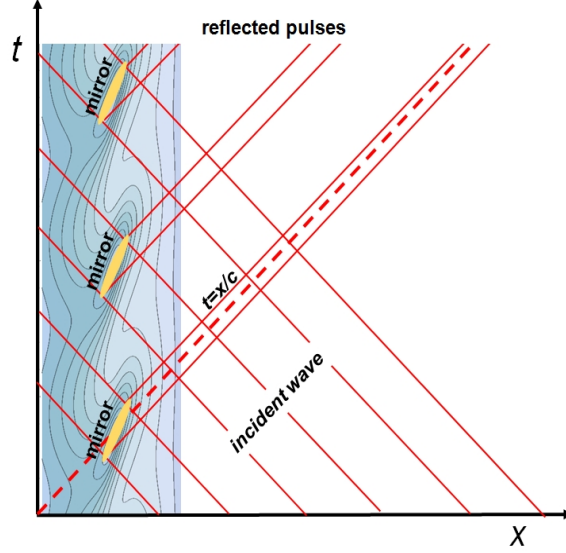


FIG. 6: Generation of ultra-short pulses in the wave reflected at periodically appearing and disappearing mirrors.

component. The ions are assumed to be at rest. Assume for the sake of simplicity that the laser pulse is given, i. e. it propagates in a plasma with a constant speed v_g without changing its shape. The plasma oscillations formed in a wake behind the laser pulse have the form of a wave in which all the functions depend on variables x and t in the combination $\zeta = x - v_{ph}t$, i. e. the wake wave propagates with the constant phase velocity v_{ph} equal to the group velocity of the driver laser pulse, v_g . The longitudinal component of the electron momentum obeys the nonlinear differential equation (e. g. see Ref. [70])

$$\left(\gamma_e - \beta_{ph} \frac{p_{||}}{m_e c}\right)'' = k_p^2 \left(\frac{p_{||}}{\gamma_e m_e c \beta_{ph} - p_{||}}\right). \quad (71)$$

Here a prime denotes differentiation with respect to the variable ζ . The electron relativistic Lorentz factor γ_e depends on the longitudinal and transverse (with respect to the wave propagation direction) components of the electron momentum, $p_{||}$ and $m_e c a_0$ as $\gamma_e = \sqrt{1 + a_0^2 + (p_{||}/m_e c)^2}$. Here it is taken into account that due to the homogeneity along the transverse direction of the configuration under consideration, the transverse component of electron momentum is proportional to the corresponding component of the normalized vector potential a_0 . Eq. (71) becomes singular when the denominator in the term on the right hand side vanishes. The singularity corresponds to the case when the electron velocity $p_{||}/m_e \gamma_e$ becomes equal to the wave phase velocity $c \beta_{ph}$, which means the wave-breaking. In a stationary wave the singularity occurs at the maximum of the electron velocity $v_m = p_{||,m}/m_e \gamma_{e,m}$. We denote the wave-breaking coordinate as ζ_m .

In order to find the structure of the singularity, we expand the electron momentum and Lorentz factor near the singularity at $\delta\zeta = \zeta - \zeta_m \rightarrow 0$, assuming smallness of $\delta p_{||} = p_{||,m} - p_{||}$, where $p_{||,m} = \beta_{ph} \sqrt{(1 + a_m^2)/(1 - \beta_{ph}^2)}$, $\delta p_{||}/p_{||,m} \ll 1$. Here $a_m = a_0(\zeta_m)$ is the vector potential value at the wavebreaking point. Keeping the main terms on both sides of Eq. (71), we obtain

$$\delta p_{||} = -m_e c \beta_{ph} \gamma_{ph}^3 \left[\frac{3\sqrt{1 + a_m^2}}{2\beta_{ph}} k_p \delta\zeta \right]^{2/3}. \quad (72)$$

For the electron velocity we have

$$v_{el} = c \beta_{ph} - c \frac{\beta_{ph}}{\gamma_{ph}} \left[\frac{3\sqrt{1 + a_m^2}}{2\beta_{ph}} k_p \delta\zeta \right]^{2/3}. \quad (73)$$

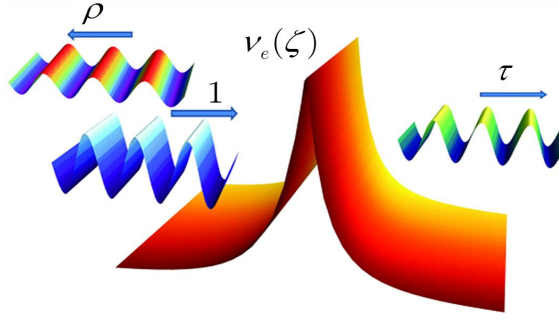


FIG. 7: Partial reflection of the electromagnetic wave incident on the moving density cusp [70, 72].

This type of singularity in the catastrophe theory is called the "cusp catastrophe" [71]. In local coordinates it can be written as a mapping $\{x\} \rightarrow \{y\}$: $y_1 = x_1$, $y_2 = x_2^3 + x_1 x_2$.

Although in the vicinity of the singularity the electron density tends to infinity as

$$n = \frac{n_0 c \beta_{ph}}{c \beta_{ph} - v_{el}} \approx n_0 \gamma_{ph} \left[\frac{3\sqrt{1 + a_m^2 \beta_{ph}}}{2k_p \delta \zeta} \right]^{2/3}, \quad (74)$$

the singularity is integrable, i.e. the breaking plasma wave contains a finite number of particles.

C. Above-Barrier Reflection from Caustics Formed by Breaking Plasma Waves

The plasma wave at the wave breaking threshold can reflect a counter-propagating electromagnetic wave due to above-barrier reflection. Following the widely used terminology, we refer to the singularities in the electron density formed during the plasma wave breaking (singularities of Lagrangian mapping) as the caustics.

In order to calculate the reflection and transmission coefficients we represent electromagnetic wave in Eqs. (37) and (38) in the form (see Refs. [70, 72])

$$a(\zeta) = \frac{1}{\sqrt{q(\zeta)}} [b_+ \exp(iW(\zeta)) + b_- \exp(-iW(\zeta))], \quad (75)$$

where the phase integral $W(\zeta)$ is given by

$$W(\zeta) = \int_0^\zeta q(z) dz. \quad (76)$$

The functions b_+ and b_- are related to the amplitudes of the reflected and transmitted waves. In the limit $\zeta \rightarrow -\infty$ the function b_+ equals the amplitude of the incident wave, which is assumed equal to unity, and $b_-(-\infty) = \rho$ corresponds to the amplitude of the reflected wave. For $\zeta \rightarrow +\infty$ the function b_+ equals the amplitude of the transmitted wave τ , and b_- vanishes (see Fig. 7). Therefore $|b_+(-\infty)|^2 = 1$, $|b_-(-\infty)|^2 = \mathbf{R}$, $|b_+(+\infty)|^2 = \mathbf{T}$ and $|b_-(+\infty)|^2 = 0$.

Since in the representation (75), the single unknown function $a(\zeta)$ has been replaced by the two unknown functions b_+ and b_- , an additional condition is necessary. We impose the condition

$$\frac{da}{d\zeta} = i\sqrt{q(\zeta)} [b_+ \exp(iW(\zeta)) - b_- \exp(-iW(\zeta))], \quad (77)$$

Eqs. (75) and (77) result in the system of equations which can be written as

$$\frac{d}{dW} \begin{pmatrix} b_+ \\ b_- \end{pmatrix} = \begin{pmatrix} 0 & S(W) \exp(-2iW) \\ S(W) \exp(2iW) & 0 \end{pmatrix} \begin{pmatrix} b_+ \\ b_- \end{pmatrix} \quad (78)$$

with

$$S(W) = \frac{1}{2} \frac{d}{dW} \ln q(\zeta(W)). \quad (79)$$

Integrating both sides of Eq. (78) and using the above formulated boundary conditions for b_+ and b_- , one can obtain the reflection coefficient ρ in the form of an infinite series [73]. In the case of weak reflection, $|\rho| \ll 1$, which requires $s^2 \gg \nu_e(\zeta)$, the reflected wave can be found within the framework of perturbation theory. This yields

$$\rho = \frac{i}{2s} \int_{-\infty}^{+\infty} \nu_e(\zeta) \exp(-2is\zeta) d\zeta. \quad (80)$$

As an important example of the calculation of the reflection coefficient, we consider a typical dependence of the electron density in the vicinity of the wavebreaking threshold in a cold plasma. This can be approximated by the expression [72]

$$\nu_e(\zeta) = \frac{g_{2/3}}{(k_p l)^{2/3} (l^2 + \zeta^2)^{1/3}}. \quad (81)$$

Here $g_{2/3} = (2/9)^{1/3} (1 + a_m^2)^{1/6} k_p^{4/3} \gamma_m^{4/3}$ is the dimensionless coefficient and the parameter $k_p l$ shows how close the wave is to the wavebreaking limit, for which $l = 0$. Calculating the integral (80) for the integrand (81), we find

$$\rho_{2/3}(s, l) = \frac{3i\sqrt{\pi}g_{2/3}l^{1/6}}{\Gamma(-2/3)k_p^{2/3}s^{7/6}} K_{1/6}(2sl). \quad (82)$$

Here $\Gamma(x)$ and $K_\nu(x)$ are the Euler gamma function and the modified Bessel function, respectively.

In the limit of relatively large l , when $sl \gg 1$, the above-barrier reflection is exponentially weak,

$$\rho_{2/3}(s, l) \approx \frac{3i\pi g_{2/3}}{\Gamma(-2/3)k_p^{2/3}s^{5/3}l^{1/3}} \exp(-2sl). \quad (83)$$

In the opposite case, when $sl \rightarrow 0$, we have a non-exponentially-small reflection [70, 72]

$$\rho_{2/3}(s) \approx \frac{3i(-2)^{2/3}\pi g_{2/3}}{k_p^{2/3}s^{4/3}\Gamma(-1/3)}. \quad (84)$$

This yields the reflection coefficient

$$\mathbf{R}_{2/3}(s) \approx \frac{2^{4/3}9g_{2/3}^2}{k_p^{4/3}s^{8/3}\Gamma^2(-1/3)}. \quad (85)$$

V. COMPACT SOURCE OF HIGH-BRIGHTNESS X-RAYS BASED ON THE MECHANISM OF A RELATIVISTIC FLYING MIRROR

A. The relativistic flying mirror in the nonlinear wake waves

Within the framework of the RFM concept (see Refs. [2, 3] and Fig. 8) the relativistic mirrors are related to the thin layers of relativistic electrons generated in nonlinear plasma waves which are excited in the plasma by a short strong laser pulse. Surfaces of constant density in the wake of nonlinear waves have the form of paraboloids of revolution [75–79]. The counter-propagating laser pulse is partially reflected from these structures. This results in a frequency upshifting of the reflected pulse, its shortening in the longitudinal direction and focusing in the transverse direction, providing the intensification of reflected radiation, despite the fact that the reflection coefficient is relatively small (see results of PIC simulations [3]).

The relativistic flying mirror with large enough reflection coefficient of the counter-propagating radiation, is formed in the process of the wake wave breaking. The phase velocity of the wake wave v_{ph} equals the group velocity of the driver laser pulse $v_g = \partial\omega/\partial k$, which, in accordance with the dispersion equation for the transverse (electromagnetic) waves, $\omega = \sqrt{k^2c^2 + \omega_{pe}^2}$, is given by formula $v_g = c\sqrt{1 - (\omega_{pe}/\omega)^2}$. In a low density plasma, where the laser frequency is much higher than the Langmuir frequency $\omega \gg \omega_{pe}$, the group velocity of electromagnetic waves is close to the speed of light in vacuum. At the threshold of wave breaking the velocity of the electrons in the wake wave becomes comparable in magnitude with the wake wave phase velocity v_{ph} , which is equivalent to the condition for the electron energy $\mathcal{E}_e = m_e c^2 \gamma_e$, where γ_e is the Lorentz factor calculated for $v_e = v_{ph}$. The wave breaking occurs if [74]

$$\gamma_e \geq \gamma_{ph} = (1 - v_{ph}^2/c^2)^{-1/2} = \omega/\omega_{pe}. \quad (86)$$

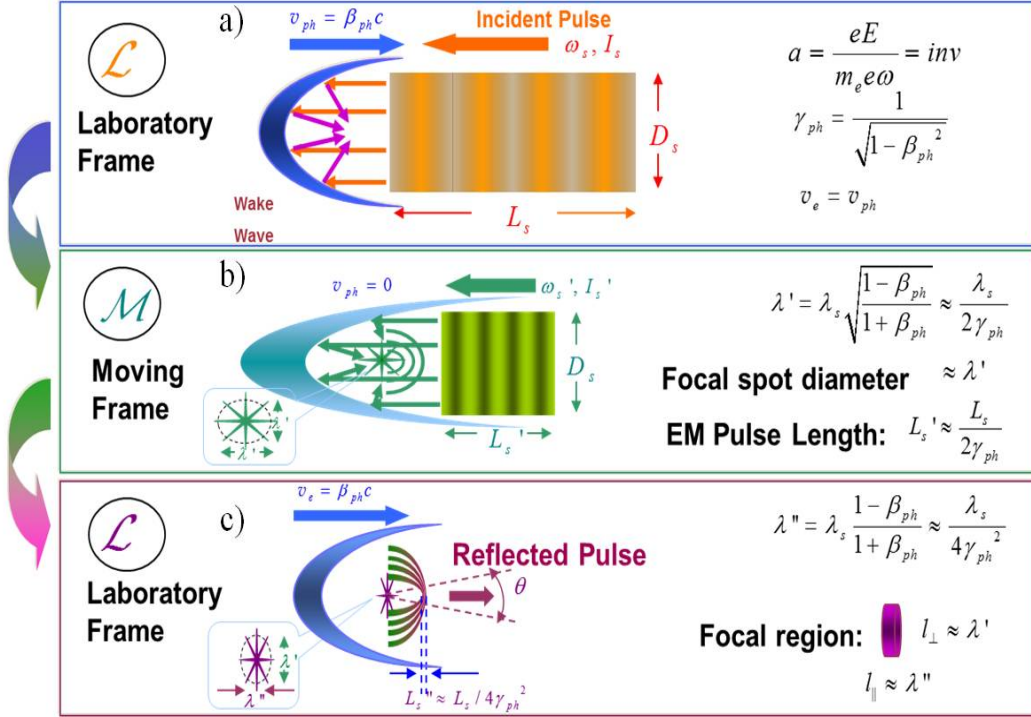


FIG. 8: The concept of flying relativistic mirror. a) Laboratory frame of reference. Before reflection from the mirror the laser pulse propagates from right to left. b) Frame of reference where the mirror is at rest. The incident laser pulse has a length $L' \approx L_s/2\gamma_M$ and wave length $\lambda' \approx \lambda_s/2\gamma_M$. After reflection from a parabolic mirror the radiation is focused to the region of size λ' . c) Laboratory frame of reference. The reflected pulse is compressed by a factor $4\gamma_M^2$; its wavelength becomes equal $\lambda'' \approx \lambda/4\gamma_M$. The moving focal region has the form of an ellipsoid with the longitudinal λ'' and transverse λ' dimension, respectively. Radiation is collimated within the angle $\theta \approx 1/\gamma_M$.

As a result of the plasma wave breaking a singularity in the distribution of electron density occurs, which breaks the geometrical optics approximation and increases the reflection coefficient. If there is no wave-breaking, the reflectivity is exponentially weak (see Eq. (83)).

In the model, when the singularity is approximated by a cusp, the reflection coefficient is given by the formula (85). In terms of the number of photons, it depends on the density of the plasma as $R_{2/3} \approx 1/\gamma_{ph}^4 = (\omega_{pe}/\omega)^4 = (n/n_{cr})^2$ in the limit $\gamma_{ph} \gg 1$. Taking into account the pulse compression in the transverse direction as a result of focusing by the parabolic mirror of the source pulse with the intensity I_s , diameter D_s , and wavelength λ_s , we obtain for reflected wave intensity

$$I_r \approx I_s \left(\frac{D_s}{\lambda_s} \right)^2 \gamma_{ph}^2. \quad (87)$$

The reflected wave energy and power equal to $\mathcal{E}_r \approx \mathcal{E}_s/\gamma_{ph}^2$ and $\mathcal{P}_r \approx \mathcal{P}_s$, respectively.

As an example, let's consider the parameters required to achieve the limit when the electron-positron pairs can be created from vacuum [19], $I_r \approx 2 \times 10^{27} \text{W/cm}^2$, for the electromagnetic wave reflected by a flying mirror. We assume that the source pulse has the power equal to 4 PW. For $\lambda_s = 1\mu\text{m}$ we obtain from Eq. (87) that $\gamma_{ph} = 60$. The wake wave breaking condition (86) yields the driver laser pulse amplitude $a_d = 11$, i.e. for the driver pulse intensity we have $I_d \approx 1.5 \times 10^{20} \text{W/cm}^2$. Since the gamma factor γ_{ph} associated with the wake wave phase velocity is equal to $\sqrt{n_{cr} a_d / n_e}$ we find from (86) that the plasma density is $\approx 3.3 \times 10^{17} \text{cm}^{-3}$. In order to excite the wake wave in the plasma with such density the laser pulse length should be equal to $l_{las} = \lambda_d \sqrt{n_{cr} a_d / 4n_e}$, i.e. $l_{las} \approx 30\mu\text{m}$ or the laser pulse duration of $\tau_{las} \approx 100\text{fs}$. Assuming the laser pulse driver diameter to be of the order of l_{las} we find the driver pulse power and energy equal to $\mathcal{P}_{las} = 15\text{PW}$ and $\mathcal{E}_{las} = 1.5\text{kJ}$, respectively.

The use of spherical Langmuir waves as a relativistic mirror can enable a much higher intensification of the reflected radiation [69]. Owing to the spherical geometry, the reflected wave with a wavelength $\approx \lambda_s/4\gamma_M^2$ is focused in the

volume $\approx \lambda_s^3/48\gamma_M^6$, that gives for the radiation intensity $I_r \approx I_s\gamma_M^4$ for the reflectron coefficient $R_{2/3} \approx 1/\gamma_M^4$. This has important implementations for studying the feasibility of experiments on the photon-photon scattering in vacuum [80].

VI. EXPERIMENTAL DEMONSTRATION OF A RELATIVISTIC FLYING MIRROR

The proof-of-principle experiments of the RFM concept have been done in Refs. [4, 5]. There the generation of soft X-rays with a narrow energy spectrum has been reported. In this experiment, two short laser pulses collided at an angle of 135° in a supersonic gas jet. The laser used in this experiment generates pulses of radiation having a wavelength 820 nm, with the energy of 210 mJ, with duration of 76 fs, i. e. it has the power of 2.75 TW. The second pulse (the source pulse) is focused providing a spatial overlay with the first pulse-driver. The beam collision configuration is not head-on in order to avoid the laser damage by the radiation propagating in the opposite direction relative to the pulse driver. The driver pulse has the intensity of 5×10^{17} W/cm². The source pulse intensity equals $\approx 10^{17}$ W/cm².

In this configuration the frequency of light reflected from the relativistic mirror should be increased by a factor $\omega_r/\omega_s \approx 3.4\gamma_{ph}^2$. The plasma density in the target is approximately equal to 5×10^{19} cm⁻³. For this plasma density the wake wave gamma factor is $\gamma_{ph} = 6.5$ and the theoretically predicted frequency upshifting factor is 140.

For the above written parameters of the laser radiation and the target plasma, the laser pulse driver excites the wake wave with a large enough amplitude exceeding the wave-breaking threshold. However, the excess over the wavebreaking threshold is not too great, and the regular wake wave structure is not destroyed. Evidence of this regime is the observation of quasi-mono-energetic spectra of electrons accelerated by the wake wave with ultrarelativistic energy of 20 MeV. Another indication of the nonlinear character of the wake is the detection of upshifted and downshifted maxima in the frequency spectrum of the laterally scattered radiation corresponding to the stimulated backward Raman scattering. In addition, an analysis of interferogram reveals the channel formation in the plasma density, which is also in accordance with the wake excitation by the laser pulse undergoing the relativistic self-focusing leading to redistribution of the electron density.

In the experiments [4, 5], the detected frequency multiplication factor is in the range from 55 to 114, corresponding to a reflected radiation wavelength from 7 to 15 nm.

Further development of the theory of relativistic flying mirror and further experiments a higher power laser have allowed to demonstrate high-efficiency regimes [6], which provides opportunities for developing highly efficient sources in the energy range corresponding to hard X-rays. In Ref. [6], a high reflection reaching the theoretical prediction has been demonstrated using the laser with an energy of 0.5 J and a power of 15 TW. In contrast to previous experiments, special efforts enabled head-on collision of the beams, which secured a three orders of magnitude higher number of reflected photons in the spectral range corresponding to soft X-rays. To detect the reflected radiation the used spectrometer had a relatively large aperture for collecting a large enough number of photons. New techniques have been implemented to perform pulse collision at a predetermined place with high accuracy at the desired time.

The number of photons of hard electromagnetic radiation, registered in the experiment [6] allows us to conclude that the agreement with theoretical predictions for the reflection coefficient, defined by the formula (85), is achieved.

In addition to the question on the relativistic mirror reflectivity it is of particular interest to determine whether the mirror has a high quality reflective surface, that is smooth enough. In the experiment presented in Ref. [6] the observed radiation in the wavelength range from 12 nm to 20 nm within the observation angles in the range from 9° to 17° has a sufficiently smooth spectral distribution. Since the frequency upshifting factor depends on the angle at which the reflected light propagates and on the local angle of reflection from the mirror surface, this shows that the radiation is reflected from a smooth surface having a curvature. This is also consistent with the predictions of the theory, which is important for further research aimed at demonstrating the sharp focusing of X-rays in order to reach the high limits of its intensity.

VII. EXTREMELY HIGH FIELD LIMITS

The purpose of further studies of the physical processes associated with relativistic mirrors is to design and build a compact source of hard electromagnetic radiation with a photon energy and intensity large enough to conduct experiments in previously inaccessible regimes of interaction of electromagnetic fields with matter. Here, we present the critical parameters that characterize the main regimes of laser-matter interaction, depending on the intensity of the electromagnetic wave (see also reviews [2, 7–10, 24]).

In the limit of extremely high wave intensity the radiation friction effects on the charged particle dynamics become dominant [81–83, 85–87]. At these limits the electron dynamics become dissipative with fast conversion of the elec-

tromagnetic wave energy to hard electromagnetic radiation, which for typical laser parameters is in the gamma-ray range [88, 89]. For laser radiation with $1\ \mu\text{m}$ wavelength the radiation friction force changes the scenario of the electromagnetic wave interaction with matter at the intensity of about $I_R \approx 10^{23}\text{W}/\text{cm}^2$. For the laser intensity close to I_R also novel physics of abundant electron-positron pair creation comes into play [90] (see [91] and [24, 92]). In this regime, the electron (positron) interaction with the electromagnetic field is principally determined by a counterplay between the radiation friction and quantum effects. The quantum electrodynamics (QED) effects weaken the electromagnetic emission by the relativistic electron resulting in the lowering of the radiation friction [93]. In an extremely high intensity electromagnetic field, vacuum shows various nonlinear quantum electrodynamics processes such as vacuum polarization, electron-positron pair plasma creation, and other properties depending on the electromagnetic field strength and distribution.

The probabilities of the processes involving extremely high intensity electromagnetic field interaction with electrons, positrons and photons are determined by several dimensionless parameters.

We consider the nonlinear electrodynamics of plasma in the limit of relativistic particle energies. As was mentioned above, the behavior of an electron in the field of an electromagnetic wave is determined by the dimensionless parameter $a = eE/m_e\omega c$, which is the normalized wave amplitude. This value is associated with a relativistic invariant,

$$a = e \frac{\sqrt{A^\mu A_\mu}}{m_e c^2}. \quad (88)$$

If $a > 1$, the electron energy becomes relativistic, which corresponds to the wave intensity above $\approx 1.37 \times 10^{18}\text{W}/\text{cm}^2$.

With further increase in the electromagnetic wave intensity, its interaction with a sufficiently dense plasma is characterized by radiation loss effects [81–83]. The energy loss rate by an electron rotating in the field of a circularly polarized wave is given by

$$\dot{\mathcal{E}}^{(-)} = \epsilon_{rad} m_e c^2 \omega a^2 (1 + a^2). \quad (89)$$

Here the dimensionless parameter

$$\epsilon_{rad} = \kappa_p \frac{2\pi r_e}{\lambda} \quad (90)$$

characterizes the the radiation losses with $\lambda = 2\pi c/\omega$ and the classical electron radius equal to $r_e = e^2/m_e c^2 \approx 2.8 \times 10^{-13}\text{cm}$. The coefficient κ_p for circularly polarized wave equals $3/8$ and for linear polarization it is $1/8$.

Because the electromagnetic wave cannot transfer energy to the particle with a rate greater than

$$\dot{\mathcal{E}}^{(+)} = eEc = m_e c^2 \omega a \quad (91)$$

the condition of the balance between incoming and radiated energy per unit time, $\dot{\mathcal{E}}^{(+)} = \dot{\mathcal{E}}^{(-)}$ yields the threshold value of the amplitude of the electromagnetic wave above which the influence of radiation losses cannot be ignored. In dimensionless form, this threshold amplitude of the wave is

$$a_{rad} = \epsilon_{rad}^{-1/3}. \quad (92)$$

For a circularly polarized wave this corresponds to the radiation intensity

$$I_R = \left(\frac{3}{2}\right)^{2/3} \frac{m_e^{8/3} c^5 \omega^{4/3}}{4\pi e^{10/3}} = 2.65 \times 10^{23} \left(\frac{1\ \mu\text{m}}{\lambda}\right)^{4/3} \frac{\text{W}}{\text{cm}^2}. \quad (93)$$

QED effects become important, when the energy of a photon generated by Thomson (Compton) scattering is of the order of the electron energy, i.e. $\hbar\omega_m \approx m_e c^2 \gamma_e$. If $\gamma_e = a_0$ this yields the quantum electrodynamics limit on the electromagnetic field amplitude, $a_0^2/a_S > 1$. Here the dimensionless parameter

$$a_S = \frac{eE_S \lambda}{2\pi m_e c^2} = \frac{m_e c^2}{\hbar\omega} = \frac{\lambda}{\lambda_C} = 4.2 \times 10^5 \left(\frac{\lambda}{1\ \mu\text{m}}\right) \quad (94)$$

is the normalized critical electric field of quantum electrodynamics [23],

$$E_S = m_e^2 c^3 / e\hbar, \quad (95)$$

with $\lambda_C = 2\pi\hbar/m_e c = 2.42 \times 10^{-10}\text{cm}$ being the Compton wavelength. The electromagnetic radiation intensity (irradiance) corresponding to the wave amplitude of a_S is

$$I_S = \frac{m_e^4 c^7}{4\pi e^2 \hbar^2} = 2.36 \times 10^{29} \frac{\text{W}}{\text{cm}^2}. \quad (96)$$

The above obtained quantum electrodynamics limit, $a_0^2/a_S > 1$, corresponds to the condition $\chi_e > 1$, where the relativistic and gauge invariant parameter χ_e ,

$$\chi_e = \frac{\sqrt{(F^{\mu\nu}p_\nu)^2}}{E_S m_e c} \approx 2 \frac{a_0}{a_S} \gamma_e, \quad (97)$$

characterizes the probability of the gamma-photon emission by the electron with 4-momentum p_ν in the field of the electromagnetic wave. The 4-tensor of the electromagnetic field is defined as $F_{\mu\nu} = \partial_\mu A_\nu - \partial_\nu A_\mu$. The quantum electrodynamics limit is reached for the electromagnetic wave intensity of the order of

$$I_Q = \frac{m_e^3 c^5 \omega}{8\pi e^2 \hbar} = 5.75 \times 10^{23} \left(\frac{1\mu\text{m}}{\lambda} \right) \frac{\text{W}}{\text{cm}^2}. \quad (98)$$

The Lorentz invariant dimensionless parameter

$$\chi_\gamma = \frac{\hbar \sqrt{(F^{\mu\nu}k_\nu)^2}}{E_S m_e c} \approx 2 \frac{a_0}{a_S^2} \frac{\omega_\gamma}{\omega} \quad (99)$$

determines the probability of the electron-positron pair creation by the photon with the energy $\hbar\omega_\gamma$ in the electromagnetic field via the Breit-Wheeler process [94, 95].

Properties of the nonlinear quantum vacuum are determined by the Poincare invariants,

$$\mathfrak{F} = (\mathbf{B}^2 - \mathbf{E}^2)/2 \quad \text{and} \quad \mathfrak{G} = (\mathbf{E} \cdot \mathbf{B}). \quad (100)$$

The probability of the electron-positron pair creation depends on

$$\mathfrak{E} = \sqrt{\sqrt{\mathfrak{F}^2 + \mathfrak{G}^2} - \mathfrak{F}} \quad \text{and} \quad \mathfrak{B} = \sqrt{\sqrt{\mathfrak{F}^2 + \mathfrak{G}^2} + \mathfrak{F}}, \quad (101)$$

which are the electric and magnetic fields in the frame of reference where they are parallel.

In the limit $\mathfrak{E}/E_S \rightarrow 1$ the electromagnetic waves can create electron-positron pairs from vacuum [21–23, 84, 98], moreover, the electromagnetic waves can interact via photon-photon collisions [85] and vacuum polarization [96]. When the parameter χ_e becomes large, the multiphoton Compton scattering results in the high energy photon generation. For $\chi_\gamma > 1$ the multiphoton Breit-Wheeler process results in electron-positron pair generation via the gamma-photon interaction with the strong electromagnetic field. The nonlinear Thomson scattering regime is realized for $a \gg 1$ with the scattering cross-section depending on the electromagnetic field amplitude. If $a_0 > a_{rad} = \varepsilon_{rad}^{-1/3}$ radiation friction effects play a key role.

The comparison of expressions given by Eqs. (93) and (98) shows that for the EM wave length equal to $\lambda \approx 0.8\mu\text{m}$ the intensities I_R and I_Q are of the same order of magnitude as has been noted in Refs. [11, 97, 99, 100]. More precisely, the curves $I_R(\omega)$ and $I_Q(\omega)$ intersect each other at the frequency equal to

$$\omega_1 = \frac{e^4 m_e}{18 \hbar^3} \quad (102)$$

corresponding to the wavelength of $\lambda_1 = 0.821\mu\text{m}$ and the photon energy of the order of 1.5 eV. This implies that QED effects in laser matter interactions soon start to be revealed at near-future super-intense laser facilities [12].

Acknowledgment

This review article is based on the materials of the plenary lecture presented at the ICPIG-2015 conference (Iasi, Romania, 2015) by S.V.B., who thanks Profs. A. Popa and V. Zamfir for organizing the event. The lecture and review present recent results obtained at JAEA.

[1] A. Einstein, Ann. Phys. (Leipzig) **17**, 891 (1905).

[2] S. V. Bulanov, T. Zh. Esirkepov, A. S. Pirozhkov, and N. N. Rosanov, Phys. Usp. **56**, 429 (2013).

[3] S. V. Bulanov, T. Zh. Esirkepov, and T. Tajima, Phys. Rev. Lett. **91**, 085001 (2003).

- [4] M. Kando, Y. Fukuda, A. S. Pirozhkov, J. Ma, I. Daito, L.-M. Chen, T. Zh. Esirkepov, K. Ogura, T. Homma, Y. Hayashi, H. Kotaki, A. Sagisaka, M. Mori, J. K. Koga, H. Daido, S. V. Bulanov, T. Kimura, Y. Kato, and T. Tajima, *Phys. Rev. Lett.* **99**, 135001 (2007).
- [5] A. S. Pirozhkov, J. Ma, M. Kando, T. Zh. Esirkepov, Y. Fukuda, L.-M. Chen, I. Daito, K. Ogura, T. Homma, Y. Hayashi, H. Kotaki, A. Sagisaka, M. Mori, J. K. Koga, T. Kawachi, H. Daido, S. V. Bulanov, T. Kimura, Y. Kato, and T. Tajima, *Phys. Plasmas* **14**, 123106 (2007).
- [6] M. Kando, A. S. Pirozhkov, K. Kawase, T. Zh. Esirkepov, Y. Fukuda, H. Kiriyaama, H. Okada, I. Daito, T. Kameshima, Y. Hayashi, H. Kotaki, M. Mori, J. K. Koga, H. Daido, A. Ya. Faenov, T. Pikuz, J. Ma, L.-M. Chen, E. N. Ragozin, T. Kawachi, Y. Kato, T. Tajima, and S. V. Bulanov, *Phys. Rev. Lett.* **103**, 235003 (2009).
- [7] G. Mourou, T. Tajima, and S. V. Bulanov, *Rev. Mod. Phys.* **78** (2006) 309.
- [8] M. Marklund and P. K. Shukla, *Rev. Mod. Phys.* **78**, 591 (2006).
- [9] S. V. Bulanov, T. Zh. Esirkepov, Y. Hayashi, M. Kando, H. Kiriyaama, J. K. Koga, K. Kondo, H. Kotaki, A. S. Pirozhkov, S. S. Bulanov, A. G. Zhidkov, N. N. Rosanov, P. Chen, D. Neely, Y. Kato, N. B. Narozhny, and G. Korn, *Plasma Physics and Controlled Fusion* **53**, 124025 (2011).
- [10] A. Di Piazza, C. Muller, K. Z. Hatsagortsyan, and C. H. Keitel, *Rev. Mod. Phys.* **84**, 1177 (2012).
- [11] S. V. Bulanov, T. Zh. Esirkepov, M. Kando, J. Koga, K. Kondo, and G. Korn, *Plasma Phys. Rep.* **41**, 1 (2015).
- [12] *ELI-Extreme Light Infrastructure Science and Technology with Ultra-Intense Lasers WHITEBOOK*, edited by G. A. Mourou, G. Korn, V. Sandner, and J. L. Collier (THOSS Media GmbH, Berlin, 2011).
- [13] S. V. Bulanov, N. M. Naumova, and F. Pegoraro, *Phys. Plasmas* **1**, 745 (1994).
- [14] L. Plaja, L. Roso, K. Rzazewski, M. Lewenstein, *J. Opt. Soc. Am. B* **15**, 1904 (1998).
- [15] N. M. Naumova, J. A. Nees, I. V. Sokolov, B. Hou, and G. Mourou, *Phys. Rev. Lett.* **92**, 063902 (2004).
- [16] Y. Nomura, R. Hoerlein, P. Tzallas, B. Dromey, S. Rykovanov, Zs. Major, J. Osterhoff, S. Karsch, L. Veisz, M. Zepf, D. Charalambidis, F. Krausz, and G. D. Tsakiris, *Nature Physics* **5**, 124 (2009).
- [17] U. Teubner and P. Gibbon, *Rev. Mod. Phys.* **81**, 445 (2009).
- [18] S. Gordienko, A. M. Pukhov, O. Shorokhov, and T. Baeva, *Phys. Rev. Lett.* **94**, 103903 (2005).
- [19] S. S. Bulanov, V. D. Mur, N. B. Narozhny, J. Nees, and V. S. Popov, *Phys. Rev. Lett.* **104**, 220404 (2010).
- [20] F. Sauter, *Z. Phys.* **69**, 742 (1931).
- [21] W. Heisenberg and H. Euler, *Z. Phys.* **98**, 714 (1936).
- [22] J. Schwinger, *Phys. Rev.* **82**, 664 (1951).
- [23] V. B. Beresteskii, E. M. Lifshitz, and L. P. Pitaevskii, *Quantum Electrodynamics* (Pergamon, New York, 1982).
- [24] S. V. Bulanov, T. Zh. Esirkepov, Y. Hayashi, M. Kando, H. Kiriyaama, J. K. Koga, K. Kondo, H. Kotaki, A. S. Pirozhkov, S. S. Bulanov, A. G. Zhidkov, P. Chen, D. Neely, Y. Kato, N. B. Narozhny, and G. Korn, *Nuclear Instr. Meth. Phys. Res. A* **660**, 31 (2011).
- [25] W. Dittrich and H. Gies, *Probing the Quantum Vacuum* (Springer, Berlin, 2000).
- [26] R. Neutze, R. Wouts, D. van der Spoel, E. Weckert, and J. Hajdu, *Nature* **406**, 752 (2000).
- [27] B. Remington, R. Drake, and D. Ryutov, *Rev. Mod. Phys.* **78**, 755 (2006).
- [28] S. V. Bulanov, T. Zh. Esirkepov, D. Habs, F. Pegoraro, and T. Tajima, *Eur. Phys. J. D* **55**, 483 (2009).
- [29] T. Zh. Esirkepov and S. V. Bulanov, *EAS Publications Series*, **58**, 7 (2012).
- [30] N. D. Birrell and P. C. W. Davies, *Quantum Fields in Curved Space* (Cambridge University Press, Cambridge, 1982).
- [31] A. A. Grib, S. G. Mamaev, and V. M. Mostepanenko, *Quantum effects in intense external fields* (Moscow, Atomizdat, 1980).
- [32] M. Lobet, M. Kando, J. K. Koga, T. Zh. Esirkepov, T. Nakamura, A. S. Pirozhkov, and S. V. Bulanov, *Phys. Lett. A* **377**, 1114 (2013).
- [33] P. Chen and G. Mourou, eprint arXiv:1512.04064.
- [34] V. I. Veksler, *Atomic Energy* **2**, 427 (1957).
- [35] T. Zh. Esirkepov, M. Borghesi, S. V. Bulanov, G. Mourou, and T. Tajima, *Phys. Rev. Lett.* **92**, 175003 (2004).
- [36] S. V. Bulanov, T. Zh. Esirkepov, M. Kando, H. Kiriyaama, and K. Kondo, *JETP* **149**, 429 (2016).
- [37] S. Kar, M. Borghesi, S. V. Bulanov, A. Macchi, M. H. Key, T. V. Liseykina, A. J. Mackinnon, P. K. Patel, L. Romagnani, A. Schiavi, and O. Willi, *Phys. Rev. Lett.* **100**, 225004 (2008).
- [38] S. Kar, K. F. Kakolee, B. Qiao, A. Macchi, M. Cerchez, D. Doria, M. Geissler, P. McKenna, D. Neely, J. Osterholz, R. Prasad, K. Quinn, B. Ramakrishna, G. Sarri, O. Willi, X. Y. Yuan, M. Zepf, and M. Borghesi, *Phys. Rev. Lett.* **109**, 185006 (2012).
- [39] I. J. Kim, K. H. Pae, C. M. Kim, H. T. Kim, J. H. Sung, S. K. Lee, T. J. Yu, I. W. Choi, C.-L. Lee, C. H. Nam, P. V. Nickles, T. M. Jeong, and J. Lee, *Phys. Rev. Lett.* **111**, 165003 (2013).
- [40] S. V. Bulanov, T. Zh. Esirkepov, M. Kando, F. Pegoraro, S. S. Bulanov, C. G. R. Geddes, C. B. Schroeder, E. Esarey and W. P. Leemans, *Phys. Plasmas* **19**, 103105 (2012).
- [41] S. S. Bulanov, E. Esarey, C. B. Schroeder, S. V. Bulanov, T. Zh. Esirkepov, M. Kando, F. Pegoraro, and W. P. Leemans, *Phys. Rev. Lett.* **114**, 105003 (2015).
- [42] S. S. Bulanov, E. Esarey, C. B. Schroeder, S. V. Bulanov, T. Zh. Esirkepov, M. Kando, F. Pegoraro, and W. P. Leemans, *Phys. Plasmas* **23**, (2016).
- [43] T. Zh. Esirkepov, S.V. Bulanov, M. Kando, A. S. Pirozhkov, and A. G. Zhidkov, *Phys. Rev. Lett.* **103**, 025002 (2009).
- [44] T. Zh. Esirkepov, J. K. Koga, A. Sunahara, T. Morita, M. Nishikino, K. Kageyama, H. Nagatomo, K. Nishihara, A. Sagisaka, H. Kotaki, T. Nakamura, Y. Fukuda, H. Okada, A. S. Pirozhkov, A. Yogo, M. Nishiuchi, H. Kiriyaama, K. Kondo, M. Kando, and S. V. Bulanov, *NIMA* **745**, 150 (2014).

- [45] L. D. Landau and E. M. Lifshitz, *The Classical Theory of Fields* (Pergamon Press, Oxford, 1980).
- [46] N. N. Rosanov, N. V. Vysotina, and A. N. Shatsev, *JETP Letters* **93**, 308 (2011).
- [47] V. V. Kulagin, V. A. Cherepenin, M. S. Hur, and H. Suk, *Phys. Plasmas* **14**, 113101 (2007).
- [48] V. V. Kulagin, V. A. Cherepenin, M. S. Hur, and H. Suk, *Phys. Rev. Lett.* **99**, 124801 (2007).
- [49] S. S. Bulanov, A. Maksimchuk, K. Krushelnick, V. Popov, V. Yu. Bychenkov, and W. Rozmus, *Physics Letters A* **374**, 476 (2010).
- [50] H.-C. Wu, J. Meyer-ter-Vehn, J. Fernandez, and B. M. Hegelich, *Phys. Rev. Lett.* **104**, 234801 (2010).
- [51] A. Andreev, K. Platonov, and S. Sadykova, *Applied Sciences* **3**, 94 (2013).
- [52] W. J. Ma, J. H. Bin, H. Y. Wang, M. Yeung, C. Kreuzer, M. Streeter, P. S. Foster, S. Cousens, D. Kiefer, B. Dromey, X. Q. Yan, J. Meyer-ter-Vehn, M. Zepf, and J. Schreiber, *Phys. Rev. Lett.* **113**, 235002 (2014).
- [53] D. Kiefer, M. Yeung, T. Dzelzainis, P. S. Foster, S. G. Rykovanov, C. L. S. Lewis, R. S. Marjoribanks, H. Ruhl, D. Habs, J. Schreiber, M. Zepf, and B. Dromey, *Nature Com.* **4**, 1763 (2013).
- [54] J. A. Wheeler, A. Borot, S. Monchoce, H. Vincenti, A. Ricci, A. Malvache, R. Lopez-Martens, F. Quere, *Nature Photonics* **6**, 829 (2012).
- [55] V. A. Vshivkov, N. M. Naumova, F. Pegoraro, and S. V. Bulanov, *Phys. Plasmas* **5**, 2727 (1998).
- [56] S. V. Bulanov, *Radiophys. Quantum Electronics* **18**, 1511 (1975).
- [57] V. I. Bratman and S. V. Samsonov, *Phys. Lett. A* **206**, 377 (1995).
- [58] S. A. Reed, T. Matsuoka, S. S. Bulanov, M. Tambo, V. Chvykov, G. Kalintchenko, P. Rousseau, V. Yanovsky, R. Kodama, D. W. Litzenberg, K. Krushelnick, and A. Maksimchuk, *Appl. Phys. Lett.* **94**, 201117 (2009).
- [59] A. S. Pirozhkov, S. V. Bulanov, T. Zh. Esirkepov, M. Mori, A. Sagisaka, and H. Daido, *Phys. Lett. A* **349**, 256 (2006).
- [60] A. S. Pirozhkov, S. V. Bulanov, T. Zh. Esirkepov, M. Mori, A. Sagisaka, and H. Daido, *Phys. Plasmas* **13**, 013107 (2006).
- [61] S. V. Bulanov, T. Zh. Esirkepov, M. Kando, S. S. Bulanov, S. G. Rykovanov, and F. Pegoraro, *Phys. Plasmas* **20**, 123114 (2013).
- [62] S. V. Bulanov, T. Zh. Esirkepov, M. Kando, J. K. Koga, and S. S. Bulanov, *Phys. Rev. E*, **84**, 056605 (2011).
- [63] V. L. Ginzburg, *Propagation of Electromagnetic Waves in Plasma* (Pergamon Press, Oxford, 1970).
- [64] S. V. Bulanov, L. M. Kovrizhnykh, and A. S. Sakharov, *Phys. Rep.* **186**, 1 (1990).
- [65] F. Brunel, *Phys. Rev. Lett.* **59**, 52 (1987).
- [66] S. Cousens, B. Reville, B. Dromey, and M. Zepf, arXiv:1602.03685v1 [physics.plasm-ph] 11 Feb 2016.
- [67] T. Tajima and J. M. Dawson, *Phys. Rev. Lett.* **43**, 267 (1979).
- [68] E. Esarey, C. B. Schroeder, and W. P. Leemans, *Rev. Mod. Phys.* **81**, 1229 (2009).
- [69] S. S. Bulanov, A. Maksimchuk, C. B. Schroeder, A. G. Zhidkov, E. H. Esarey, and W. P. Leemans, *Phys. Plasmas* **19**, 020702 (2012).
- [70] A. V. Panchenko, T. Zh. Esirkepov, A. S. Pirozhkov, M. Kando, F. F. Kamenets, and S. V. Bulanov, *Phys. Rev. E*, **78**, 056402 (2008).
- [71] T. Poston and I. Stewart, *Catastrophe Theory and Its Applications* (London: Pitman, 1978).
- [72] S. V. Bulanov, T. Zh. Esirkepov, M. Kando, J. Koga, A. S. Pirozhkov, T. Nakamura, S. S. Bulanov, C. B. Schroeder, E. Esarey, F. Califano, and F. Pegoraro, *Phys. Plasmas* **19**, 113103 (2012).
- [73] M. V. Berry, *J. Phys. A* **15**, 3693 (1982).
- [74] A. I. Akhiezer and R. V. Polovin, *Sov. Phys. JETP* **3**, 696 (1956).
- [75] S. V. Bulanov and A. S. Sakharov, *JETP Lett.* **54**, 203 (1991).
- [76] S. V. Bulanov, F. Pegoraro, A. M. Pukhov, and A. S. Sakharov, *Phys. Rev. Lett.* **78**, 4205 (1997).
- [77] A. Pukhov and J. Meyer-Ter-Vehn, *Appl. Phys. B* **74**, 355 (2002).
- [78] N. H. Matlis, S. Reed, S. S. Bulanov, V. Chvykov, G. Kalintchenko, T. Matsuoka, P. Rousseau, V. Yanovsky, A. Maksimchuk, S. Kalmykov, G. Shvets, and M. C. Downer, *Nature Physics* **2**, 749 (2006).
- [79] A. Buck, M. Nicolai, K. Schmid, C. M. S. Sears, A. Savert, J. M. Mikhailova, F. Krausz, M. C. Kaluza, and L. Veisz, *Nature Physics* **7**, 543 (2011).
- [80] J. K. Koga, S. V. Bulanov, T. Zh. Esirkepov, A. S. Pirozhkov, M. Kando, and N. N. Rosanov, *Phys. Rev. A*, **86**, 053823 (2012).
- [81] Ya. B. Zel'dovich, *Sov. Phys. Usp.* **18**, 79 (1975).
- [82] A. Zhidkov, J. Koga, A. Sasaki, and M. Uesaka, *Phys. Rev. Lett.* **88**, 185002 (2002).
- [83] S. V. Bulanov, T. Zh. Esirkepov, J. Koga, and T. Tajima, *Plasma Phys. Rep.* **30**, 21 (2004).
- [84] R. Ruffini, G. Vereshchagin, and S. S. Xue, *Physics Reports* **487**, 1 (2010).
- [85] J. K. Koga, T. Zh. Esirkepov, and S. V. Bulanov, *Phys. Plasmas* **12**, 093106 (2005).
- [86] A. Zhidkov, S. Masuda, S. S. Bulanov, J. Koga, T. Hosokai, and R. Kodama, *Phys. Rev. STAB* **17**, 054001 (2014).
- [87] A. Thomas, C. Ridgers, S. S. Bulanov, B. J. Griffin, and S. Mangles, *Phys. Rev. X* **2**, 041004 (2012).
- [88] C. P. Ridgers, C. S. Brady, R. Duclous, J. G. Kirk, K. Bennett, T. D. Arber, A. P. L. Robinson, and A. R. Bell, *Phys. Rev. Lett.* **108**, 165006 (2012).
- [89] T. Nakamura, J. K. Koga, T. Zh. Esirkepov, M. Kando, G. Korn, and S. V. Bulanov, *Phys. Rev. Lett.* **108**, 195001(2012).
- [90] A. R. Bell and J. G. Kirk, *Phys. Rev. Lett.* **101**, 200403 (2008).
- [91] A. M. Fedotov, N. B. Narozhnyi, G. Mourou, and G. Korn, *Phys. Rev. Lett.* **105**, 080402 (2010).
- [92] S. S. Bulanov, T. Esirkepov, J. Koga, A. Thomas, and S. V. Bulanov, *Phys. Rev. Lett.* **105**, 220407 (2010).
- [93] J. Schwinger, *Proc. Natl. Acad. Sci. U.S.A.* **40**, 132 (1954).
- [94] G. Breit and J. A. Wheeler, *Phys. Rev.* **46**, 1087 (1934).
- [95] A. I. Nikishov and V. I. Ritus, *Sov. Phys. Uspekhi* **13**, 303(1970).

- [96] N. N. Rosanov, JETP Lett. **88**, 501 (2008).
- [97] C. S. Brady, C. P. Ridgers, T. D. Arber, A. R. Bell, and J. G. Kirk, Phys. Rev. Lett. **109**, 245006 (2012).
- [98] V. S. Popov, V. D. Mur, N. B. Narozhnyi, and S. V. Popruzhenko, JETP **149**, 623 (2016).
- [99] T. Zh. Esirkepov, S. S. Bulanov, J. K. Koga, M. Kando, K. Kondo, N. N. Rosanov, G. Korn, and S. V. Bulanov, Phys. Lett. A **379**, 2044 (2015).
- [100] M. Jirka, O. Klimo, S. V. Bulanov, T. Zh. Esirkepov, E. Gelfer, S. S. Bulanov, S. Weber, and G. Korn, Phys. Rev. E **93**, 023207 (2016).